SANDIA REPORT

SAND90—0312 • UC—528
Unlimited Release
Printed December 1990

Mass and Performance Estimates for 5 to 1000 kW(e) Nuclear Reactor Power Systems for Space Applications

Louis O. Cropp, Donald R. Gallup, Albert C. Marshall

Prepared by
Sandia National Laboratories
Albuquerque, New Mexico 87185 and Livermore, California 94550
for the United States Department of Energy
under Contract DE-AC04-76DP00789

Issued by Sandia National Laboratories, operated for the United States Department of Energy by Sandia Corporation.

Available to DOE and DOE contractors from
Office of Scientific and Technical Information
PO Box 62
Oak Ridge, TN 37831

Prices available from (615) 576-8401, FTS 626-8401

Available to the public from
National Technical Information Service
US Department of Commerce
5285 Port Royal Rd
Springfield, VA 22161

NTIS price codes
Printed copy: A05
Microfiche copy: A01

Accession Number: 4425

Publication Date: Dec 01, 1990

Title: Mass and Performance Estimates for 5 to 1000 kW(e) Nuclear Reactor Power Systems for Space Applications

Personal Author: Cropp, L.O.; Gallup, D.R.; Marshall, A.C.

Corporate Author Or Publisher: Sandia National Laboratories, PO Box 5800, Albuquerque, NM 87185
Report Number: SAND90-0312

Report Prepared for: US Department of Energy, Office of Scientific and Technical Information, PO Box 62, Oak Ridege, TN 37831

Descriptors, Keywords: Nuclear Reactor Power System Space Applications Sandia

Pages: 00068

Cataloged Date: Mar 31, 1993

Contract Number: DE-AC04-76DP00789

Document Type: HC

Number of Copies In Library: 000001

Record ID: 26585

SAND90-0312
Unlimited Release
December 1990

Distribution
Category UC-528

MASS AND PERFORMANCE ESTIMATES FOR 5 TO 1000 kW(e) NUCLEAR REACTOR POWER SYSTEMS FOR SPACE APPLICATIONS*

Louis O. Cropp
Donald R. Gallup
Albert C. Marshall
Sandia National Laboratories
P. O. Box 5800
Albuquerque, NM 87185

ABSTRACT

Masses and radiator areas of typical space nuclear power concepts are estimated as a function of the continuous electrical power required during a ten-year mission. Results are presented as a function of power level in the range of 5 to 1000 kW electrical. Three general reactor types will be discussed: (1) the radiatively cooled Star-C reactor technology with thermionic conversion external to the core; (2) liquid metal cooled technology with pin-type thermionic fuel element conversion in the core; and (3) the liquid metal cooled SP-100 reactor technology with thermoelectric, Brayton, Stirling, and Rankine conversion systems. Mass estimates include all satellite subsystems except the payload itself. Area estimates include radiators to dump waste heat from the power conversion, power conditioning, power transmission, and reactor control subsystems but not the payload. All system components utilize near-term technology with the exception of the SP-100 Rankine and refractory Stirling concepts.

* This work was performed at Sandia National Laboratories, which is operated for the U. S. Department of Energy under contract number DE-AC04-76DP00789.

This page intentionally left blank.

TABLE OF CONTENTS

This page intentionally left blank.

LIST OF FIGURES

Acknowledgements

Mr. Steven L. Hudson and Mr. Richard E. Pepping of Sandia National Laboratories, Mr. David T. Furgal of G2 vanTel, Ltd., and Ms. Barbara I. McKissock of NASA's Lewis Research Center provided valuable input to this paper; Mr. Hudson by performing analyses of the liquid metal Rankine turboalternator, heat transport loops, and boom structure; Mr. Pepping by supplying a satellite systems perspective in helping to define the ground rules for this study and by identifying the effects of the natural environment on the systems; Mr. Furgal by specifying the power conditioning equipment and transmission lines and developing mass and performance algorithms for them; and Ms. McKissock by providing mass algorithms for the Stirling engine, heat exchangers, heat transport loops, and liquid metal vapor separators.

Executive Summary

The design of nuclear reactors for space power applications is influenced by many technical, programmatic, and political considerations. The desire to develop long-lived, safe, reliable power sources is paramount and has been the subject of many papers. Those needs and some of the more important reactor characteristics are briefly mentioned here but this report focuses on how the mass and radiator area of the leading near-term reactor power system concepts vary over the range of 5 to 1000 kW(e).

There are at least four competing technologies to choose from in United States within the 5 to 1000 kW(e) range: (1) Out-of-Core Thermionic Reactor (OTR) power systems, (2) Thermionic Fuel Element, (3) Gas-cooled reactors with Brayton turbines, and (4) SP-100. Additional concept design and development work will have to be done utilizing the first three technologies before any advantages over SP-100, the technology presently being pursued in the U. S., can be confirmed. Of the concepts listed above, the OTR, Thermionic Fuel Element, and SP-100 thermoelectric concepts offer static energy conversion systems while gas cooled Brayton concepts and SP-100 with Stirling, Brayton, or Rankine conversion subsystems are dynamic. All of the concepts use coolant loops, except STAR-C which transfers heat from the core by conduction and radiation. Those which use coolant loops utilize a liquid metal coolant except for the gas Brayton concept. The thermionic fuel element concepts offer a conversion technique and choices of liquid metal coolants that are very different from the various SP-100 concepts. (Note: Due to financial constraints, gas-cooled reactors with Brayton conversion systems are not addressed in this study.)

All of the power systems we considered utilize near-term technology with two exceptions; the SP-100 Rankine and the SP-100 Refractory Metal Stirling Engine concepts. The Rankine conversion technology is further out in time because it requires two-phase flow in a micro-gravity environment. In addition, turbines and vapor separators for use with liquid metals in the Rankine turbine concept and refractory metal components for the free piston Stirling engine must be developed and proven reliable for long term use at high temperatures. These are issues that will not be resolved for several years. It is also important to recognize that technology risk and development costs are not the same even among systems labeled "near-term".

In any comparative systems analysis it is absolutely essential to pick a common set of ground rules against which to assess the various concepts. When time and

resources are limited, as in this case, these ground rules must be simplified to the point where they address only the major issues. As a result, we have performed top level system mass, area, and performance analyses based on the ground rules shown in Table 3.1. Mass estimates include all satellite subsystems except the payload but do not include the means to survive enemy attack. Since many of the concepts are not well defined and we have no specific satellite to serve as a guide for power system integration, we cannot determine system volumes at launch and during operation. Instead, we present areas of the radiators required to dump waste heat as a general indication of those volumes. Area estimates include radiators for power conversion, power conditioning, and reactor control subsystems but not the payload. We have optimized component performance within the constraint of minimizing overall power system mass for all of the more massive components. Our mass and area results may not be completely representative of real systems because many design details are unknown at this time. They should however provide good relative comparisons among the various concepts. Special care was taken to treat the SP-100 Thermoelectric system in identical fashion to the other concepts since it has received more design funding and has therefore identified many additional contributors to total system mass. We believe our approach is reasonable because our results agree well with those obtained from the SP-100 program for the SP-100 thermoelectric and innovative SP-100 concepts.

Based on our mass and area estimates, which do not include the means to survive hostile threats, there is no compelling reason to choose one nuclear power system technology over another at power levels below 40 kW(e) until requirements become more firmly established. Differences in volume at launch and during operation may be more important than mass differences at the lower power levels. However, differences in power system masses become more significant as the required power increases further and further beyond the 40 to 60 kW(e) range.

Satellite designers must understand how the total system mass, volume at launch, and volume during operation change with the amount of power required by different satellites. These are major factors in determining cost and operational capabilities and the power system's contribution to satellite mass and volume must be well understood. Since the required technology is not available, any proposed U.S. reactor will require many years for development, and the costs will be significant. This means the technology selected will be expected to satisfy U.S. operational needs for 30 or 40 years to amortize the costs. During this

time, new civilian and military missions could evolve and the required power levels are not well known this far in the future. As a result, space reactors should have the flexibility to meet different power requirements in successive designs without excessive increases in specific mass (i.e., mass per unit of electrical power) or volume. Since our results show that the various concepts differ greatly in their ability to provide such flexibility, realistic appraisals of the range of future power requirements are essential to choosing the correct reactor technologies for space missions. Even then, other power system characteristics will be equally important. This is especially true if, as we expect, the power system will account for only 10 to 20% of the satellite's total mass and 25 to 50% of its area.

Until requirements are more firmly defined, especially those dealing with survivability, and power systems are designed to meet these and many other specific satellite integration requirements, comparisons of power system concepts will remain mostly a matter of conjecture because many system attributes, including mass, may be altered dramatically by these requirements.

1.0 Introduction

In the United States, requirements for long-term continuous power in space have been modest and have been fulfilled using solar and radioisotope power sources. Future requirements fall in the range of 5 to 1000 kW(e) where nuclear reactors could provide advantages in many applications. In 1983, the United States embarked on a program, called the SP-100, to develop a space reactor technology capable of providing tens to hundreds of kilowatts of electrical power with the reference design to provide 100 kW(e). During that time the Air Force continued to examine its military mission requirements and concluded that reactors capable of providing 5 to 40 kW(e) may serve Air Force needs for many years (Ref. 2). As a result, reactor concepts other than the SP-100 which have been proposed for this low end of the power range have attracted attention within the Air Force. This in turn has raised questions concerning similarities and differences in military and civilian requirements, possible needs for separate military and civilian space reactor programs and whether separate programs would lead to similar or different technologies. The requirements are still evolving as are the concepts being proposed and this leads to continued evaluation of the direction and composition of the United States' space power program: a process which we think requires much more information concerning both requirements and reactor designs before rational changes can be considered.

There are at least four competing nuclear technologies to choose from in United States within the 5 to 1000 kW(e) range: (1) Out-of-Core Thermionic Reactors (OTRs), (2) Thermionic Fuel Element (TFE) (3) gas-cooled reactors with Brayton turbines, and (4) SP-100. Additional concept design and development work will have to be done utilizing the first three technologies before any advantages over SP-100, the technology presently being pursued in the U.S., can be confirmed. Of the concepts listed above, the OTR, TFE, and SP-100 thermoelectric concepts offer static energy conversion systems while gas cooled Brayton concepts and SP-100 with Stirling, Brayton, or Rankine conversion subsystems are dynamic. All of the concepts use coolant loops, except STAR-C which transfers heat from the core by conduction and radiation. Those which use coolant loops utilize a liquid metal coolant except for the gas Brayton concept. The thermionic fuel element concepts offer a conversion technique and choices of liquid metal coolants that are very different from the various SP-100 concepts. (Note: Due to financial constraints, gas-cooled reactors with Brayton conversion systems are not addressed in this study.)

The objective of our analyses was to compare the total masses and areas of the various power system concepts. These are the only tangibles we can compare at this juncture because the concepts are in very different stages of development, some being no more than conceptual ideas produced by a few months of study while others have been through the first design iterations. In addition, we have no specific satellite to serve as a guide for system integration as is necessary to determine volumes of the total system at launch and during operation. There are other important issues such as safety, reliability, launch costs, development costs and schedules, etc. and we allude to some of these to point out that mass and radiator areas are only a subset of the total that must be considered in the final selection process.

A general description of each of the power system concepts we analyzed in this study is given in Chapter 2. Chapter 3 lays out the ground rules that were used to obtain the system mass and area estimates. The results of the analyses are presented in Chapter 4 and the conclusions are given in Chapter 5.

2.0 Power System Descriptions

A general description of the six basic power system concepts that we analyzed is given below. The descriptions are intentionally short, because details are not available for most of the concepts.

2.1 The OTR Power System

The Space Thermionic Advance Reactor-Compact (STAR-C) concept (Ref. 2), which is a specific version of an OTR power system, is depicted in Figure 1. This concept consists of a radiatively cooled reactor core that is surrounded by flat plate thermionic devices, located in the reflector region. Its two major advantages are that it does not have a coolant loop, which increases reliability and safety, and it has a small radiator. Its major disadvantage is that it becomes increasingly heavy at power levels above about 50 kWe.

STAR-C uses a solid core composed of segmented, annular fuel plates that are supported by graphite trays. Each fuel plate is made up of six, pie-shaped, Uranium Dicarbide segments fully enriched in U-235. The graphite trays are coated with Niobium Carbide to suppress carbon sublimation, which could result in carbon attack on the emitters of the thermionic devices. The reactor core is built by stacking the graphite trays and fuel plates; the number of fuel-tray assemblies being dictated by the power level. A 10 kW(e) system has a core that is approximately 26 cm in diameter and 48 cm long. The thickness of the trays can be varied to improve the uniformity of the power profile. Heat generated in the reactor core is conducted radially outward to the core surface where it is radiated to thermionic devices surrounding the core. During operation, the maximum core and core surface temperatures are expected to be approximately 2300K and 2000K respectively.

The thermionics, located in the radial reflector, collect heat radiated across a gap from the core. Nominal operating temperature of the emitter is 1860K. The collector is cooled by an integral heat pipe which conducts heat to the system radiator surrounding the reactor. The radiator is sized so that the collector operating temperature is 1000K. Under these conditions, the efficiency of the thermionic devices is approximately 14%. When the other electrical losses are considered, the overall system efficiency is approximately 12%. The thermionic devices are connected in a series/parallel network to minimize the impact of device failures on the total system electrical output.

Reactor control is accomplished by movable rods located in the radial reflector. The rods consist of a Boron Carbide poison section and a Beryllium reflector section. When the reactor is shut down, the poison section of the rod is located in the reflector. To start the reactor, the rods are moved upward to place the Beryllium section in the reflector.

Radiation protection for the payload is provided by a separation boom, a Lithium Hydride neutron shield, and a Zirconium Hydride gamma shield. The boom length and shield thicknesses are optimized based on system mass.

The mass of the STAR-C power system in the 10 to 50 kWe range can be decreased significantly by making some minor changes in the concept. These changes consist primarily of optimizing the core length to diameter ratio and maximizing the ratio of the inner to outer fuel radius (Ref. 3). This "optimized OTR" is included in the mass comparisons in Chapter 4.

2.2 TFE Based Power Systems

Three in-core thermionic reactor concepts, which are based on the thermionic fuel element were evaluated in this study. These concepts include (a) an all-TFE reactor (Ref. 4), (b)a moderated TFE reactor (TOPAZ, Ref. 5), and (c) a TFE reactor with SNAP driver fuel (Ref. 6). All of these concepts incorporate rotating reflector/control drums within the pressure vessel, surrounding the core.

The TFE based reactor concepts employ cylindrical fuel/converter elements that are stacked on end in a manner analogous to dry cells in a flashlight (Figure 2.2). The converter stack is encased in a metallic cladding to form a thermionic fuel element (TFE). Each cell consists of a stack of annular Uranium di-oxide fuel pellets surrounded by a tungsten emitter, a cesium vapor-filled gap, a collector and an insulator sheath (Figure 2.3). During power operation, heat from the nuclear fuel boils electrons off the emitter surface (~1800 K) across the interelectrode gap to the cooler (~1000 K) collector surface. The voltage potential between the emitter and collector is used to drive the current through the electrical load. Total power system efficiencies are typically on the order of 8.5%.

Waste heat is carried from the cladding surface to a radiator by a flowing NaK coolant. Thermoelectromagnetic pumps and the SP-100 radiator design were assumed in our analysis. Radiation shields consisting of Zirconium-Hydride plus Lithium Hydride layers and Tungsten plus Lithium Hydride layers were both considered in our calculations.

The all-TFE concept (Figure 2.4) is a fast reactor with no moderator or driver fuel. This concept is more suitable for higher power levels (≥100 KWe) since the critical mass requirements are relatively high. The absence of a moderator or driver fuel permits coolant temperatures up to 1000 K or more.

The TOPAZ reactor (Figure 2.5) incorporates a Zirconium-Hydride moderator between the fuel elements to reduce critical mass requirements. The presence of a Zirconium-Hydride moderator limits coolant temperatures to about 900 K. Because the thermal neutron cross-section of natural tungsten is too high to permit its use in a moderated reactor, Tungsten-184 would have to be used for emitter fabrication. Except for this substitution, the required thermionic fuel element design is virtually identical to the thermionic fuel element for the all-thermionic fuel element concept.

In the driver fuel concept (Figure 2.6), auxiliary non-thermionic fuel elements are used to achieve criticality. The concept uses SNAP-reactor-type fuel elements (Zirconium hydride with 15 w/o uranium loading) as the driver fuel elements. Nuclear heat produced in the driver fuel is not utilized for electrical power; consequently this approach is somewhat less efficient than the other two thermionic fuel element concepts. The use of SNAP fuel also limits coolant temperatures to about 900 K.

2.3 SP-100

The SP-100 thermoelectric power system (Ref. 7) shown in Figure 2.7 converts heat generated within a compact high-temperature fast-spectrum reactor directly into electricity through the use of thermoelectric conversion. The net efficiency for this system is about 4%. Although this is quite low, the system mass in the 100 kWe range is moderate, and no moving components are required for power conversion or fluid flow.

For the reference 100 kWe design being pursued in the on-going SP-100 thermoelectric program, the reactor core is about 35 cm in length and diameter and consists of bundles of 0.77 cm diameter fuel pins contained in a niobium alloy pressure vessel (see Figure 2.8). The fuel pins are made up of uranium nitride fuel pellets within a rhenium-lined niobium alloy cladding. Beryllium oxide reflector segments surround the core circumference and are external to the pressure vessel. The reflector elements are hinged at one end and their radial position is adjusted at the opposite end of the reflector to control reactivity by regulating neutron leakage out of the core. In-core safety rods are also provided to maintain the reactor in the shutdown

condition during potential accident scenarios. A reentry heat shield surrounds the reactor to prevent core disruption during an accidental reentry.

The payload and power system electronics are protected from reactor gamma and neutron radiation by a shadow shield at the aft end of the reactor. The shield consists of layers of beryllium, tungsten, and lithium hydride. Additional attenuation of the dose to the payload is achieved by separating the payload from the reactor by a boom. A flowing lithium coolant is used in the primary heat transport system to transfer heat from the reactor fuel pins to the thermoelectric power conversion modules. The primary heat transport system is arranged into twelve identical heat transport loops and one separate auxiliary cooling loop. The primary heat transport loop consists of piping, accumulators, thermoelectromagnetic pumps, thaw heat pipes, micrometeoroid protection, and other hardware. Core coolability during a loss-of-coolant accident is insured by the auxiliary coolant loop which consists of in-core bayonet cooling tubes dispersed throughout the core.

The thermoelectric power conversion modules convert the thermal energy, carried from the reactor by the flowing lithium coolant, directly to electric energy. Silicon germanium thermoelectric cells are built up into modules which are conductively coupled to the primary loop lithium heat exchanger through compliant pads. The heat rejection subsystem is also made up of twelve identical modules incorporating a lithium coolant and thermoelectromagnetic pumps. Waste heat is carried by the flowing lithium coolant to the conical radiator, which is located between the shield and payload. Finned, titanium heat pipes attached to the lithium radiator ducts reject the waste heat to space via radiation.

At power levels below about 30 kWe, the secondary coolant loop can be eliminated by placing heat pipes on the cold side of the thermoelectric converters (Ref. 6). By eliminating the secondary loop, the power system mass can be reduced by 10 to 20%. This design is called the innovative SP-100.

2.4 SP-100 With Stirling Power Conversion

For this study, the SP-100 Stirling power system shown in Figure 2.9 and Figure 2.10 is assumed to be composed of the same components as the SP-100 thermoelectric power system except for the method used to convert thermal energy to electric energy. We assumed that the SP-100 Stirling power system uses six free-piston Stirling engines (Figure 2.11)

with linear alternators instead of thermoelectric modules. As explained in the Ground Rules reliability section, six engines are required to provide 20% redundancy. Based on information from NASA (Ref. 9) we assumed that the specific mass of the Stirling engines is constant with power level. Our calculations assumed the use of two different free piston Stirling engines; one a superalloy engine with temperature limits of 1050 K, and the other a refractory engine which might permit operation up to 1350 K. Heat energy from the reactor is carried to the Stirling engines by a flowing lithium coolant. Helium is the engine working fluid. Since the Stirling cycle approaches a Carnot cycle, high cycle efficiencies, typically around 30%, are achievable. System optimization for refractory Stirling power systems results in effective heat rejection temperatures of only about 620 K. For superalloy engines this temperature is about 520K. These low heat rejection temperatures require systems with relatively large radiators, but because the cycle efficiency is so much higher, they are still smaller than the thermoelectric system radiators.

2.5 SP-100 With Rankine Power Conversion

Here, as with the SP-100 Stirling power system, we assumed that six conversion systems would be used for reliability and that the specific mass of the conversion system was constant with power level. This potassium Rankine system utilizes a primary lithium heat transport loop, as depicted in Figure 2.12, to deliver heat from the nuclear reactor core to the potassium working fluid of the Rankine cycle via the intermediate heat exchanger. A vapor separator in the potassium loop is located at the outlet to the intermediate heat exchanger and provides nearly 100% quality vapor to the turbine inlet. The potassium vapor is then expanded through the axial flow turbine and completely condensed in the condenser heat exchanger. Waste heat is radiated to space with a heat pipe radiator that is directly connected to the condenser heat exchanger. The liquid potassium is finally pumped back through the intermediate heat exchanger to complete the cycle.

The lithium heat transport loop and nuclear reactor core are similar in construction to the SP-100 thermoelectric and Stirling power systems. Electrical energy is provided by a turbine driven iron-core generator, with a net system efficiency of about 22% for operating temperatures between 1300K (boiling) and 800K (condensing). Most materials of construction are expected to be nickel superalloys at these temperatures, although refractory based alloys may also be considered.

2.6 SP-100 With Brayton Power Conversion

The SP-100 nuclear reactor and primary heat transport loop were also mated with a simple Brayton power conversion cycle. Again, six power conversion units (each unit composed of a compressor, turbine, and alternator on the same rotating shaft) were provided for the required redundancy. Thermal energy from the lithium primary heat transport loop was provided to the helium-xenon working fluid of the Brayton cycle by the intermediate heat exchanger. The high pressure He-Xe enters the turbine at temperatures of about 1345K, expands through the turbine, is cooled in the heat pipe radiator, and is recompressed before entering the intermediate heat exchanger to complete the cycle. Turbine work provided by the expanding gas powers both the compressor and alternator. No recuperator is employed in this simple Brayton cycle. With compressor and turbine efficiencies of 85% and 90%, respectively, the overall cycle efficiency is about 22% to obtain the minimum total power system mass.

The Brayton cycle upper temperature limit would allow fabrication from nickel alloys for most components, although the intermediate heat exchanger is assumed to be made of niobium allow. The turbines do not have blade cooling at these temperatures, although center-shaft and disk cooling would be required to provide less massive rotating parts.

The SP-100 Brayton flow diagram is the same as the SP-100/Rankine flow diagram (Figure 2.12) with two exceptions. First, the Brayton system does not have a vapor separator. Second, the Brayton system has a compressor rather than a pump, and the compressor is on the same shaft as the turbine.

2.7 Electrical Subsystems

The flow of electrical power is shown in Figure 2.13. Heat from the reactor is converted to ac or dc electrical power by the power conversion subsystem as described in the Sections 2.1 through 2.6. The electrical power is then carried down the separation boom via a transmission line and converted to the appropriate voltages by the power conditioning subsystem.

The transmission line is sized to have a minimal mass while at the same time having a reasonably small power loss. This is achieved by calculating the mass, power loss, and temperature of the transmission line and, using standard wire size data, determining the optimum cable diameter and

number of conductors as a function of power level, boom length, operating voltage, conductor material properties, etc.

For power system concepts with conversion devices that supply dc power, the power conditioner is a dc to dc converter utilizing power MOSFET switch technology operating at 20 kHz. Separate converter modules supply each of the required voltage outputs. For concepts with conversion devices which produce ac power, the power conditioner consists of a rectifier/filter circuits for each output voltage. This assumes that a tapped alternator having the necessary number of output windings is used. The electronics technology used for the power conditioning subsystems is described in Reference 10.

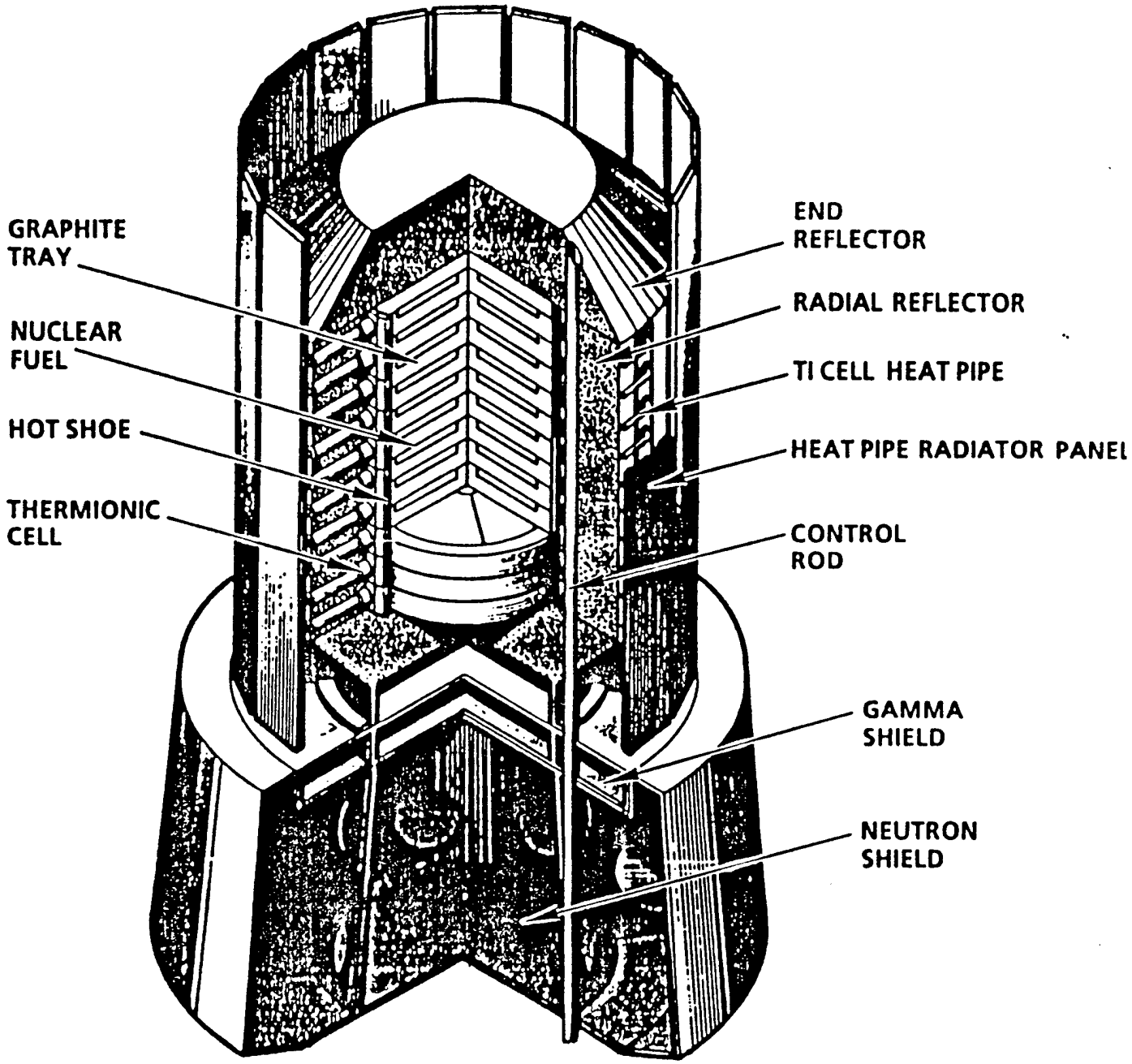

Figure 2.1: Schematic Diagram Of The STAR-C Space Nuclear Reactor (Ref.2).

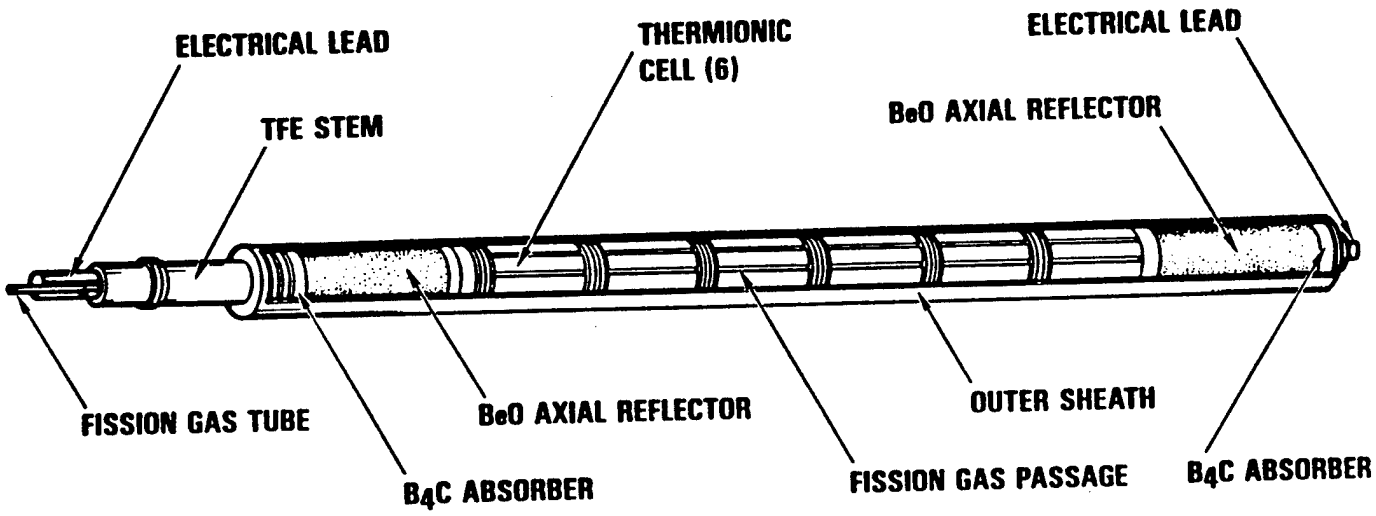

Figure 2.2: Schematic Diagram Of A Thermionic Fuel Element (Ref. 4).

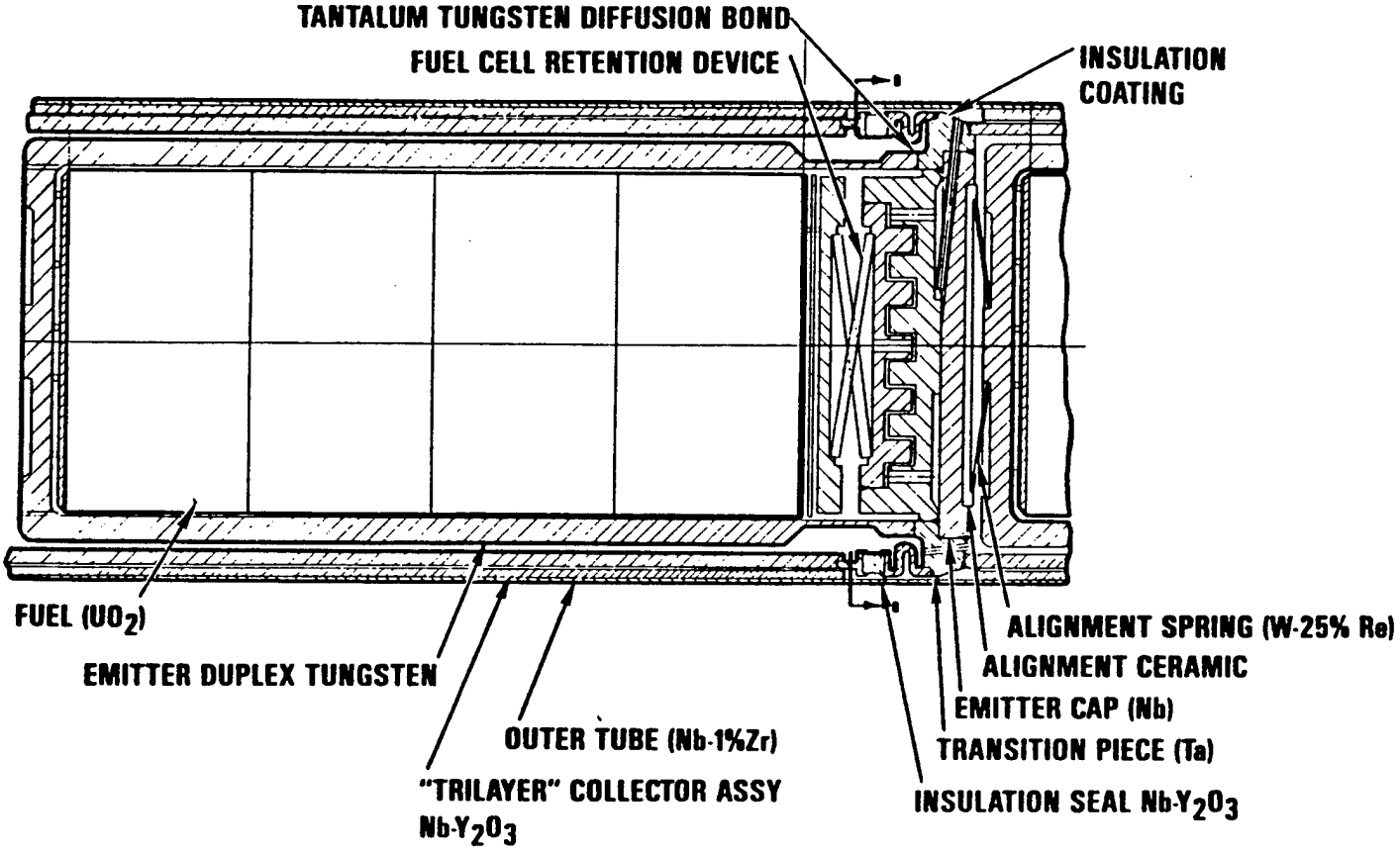

Figure 2.3: Schematic Diagram Of A Thermionic Fuel Cell (Ref. 4).

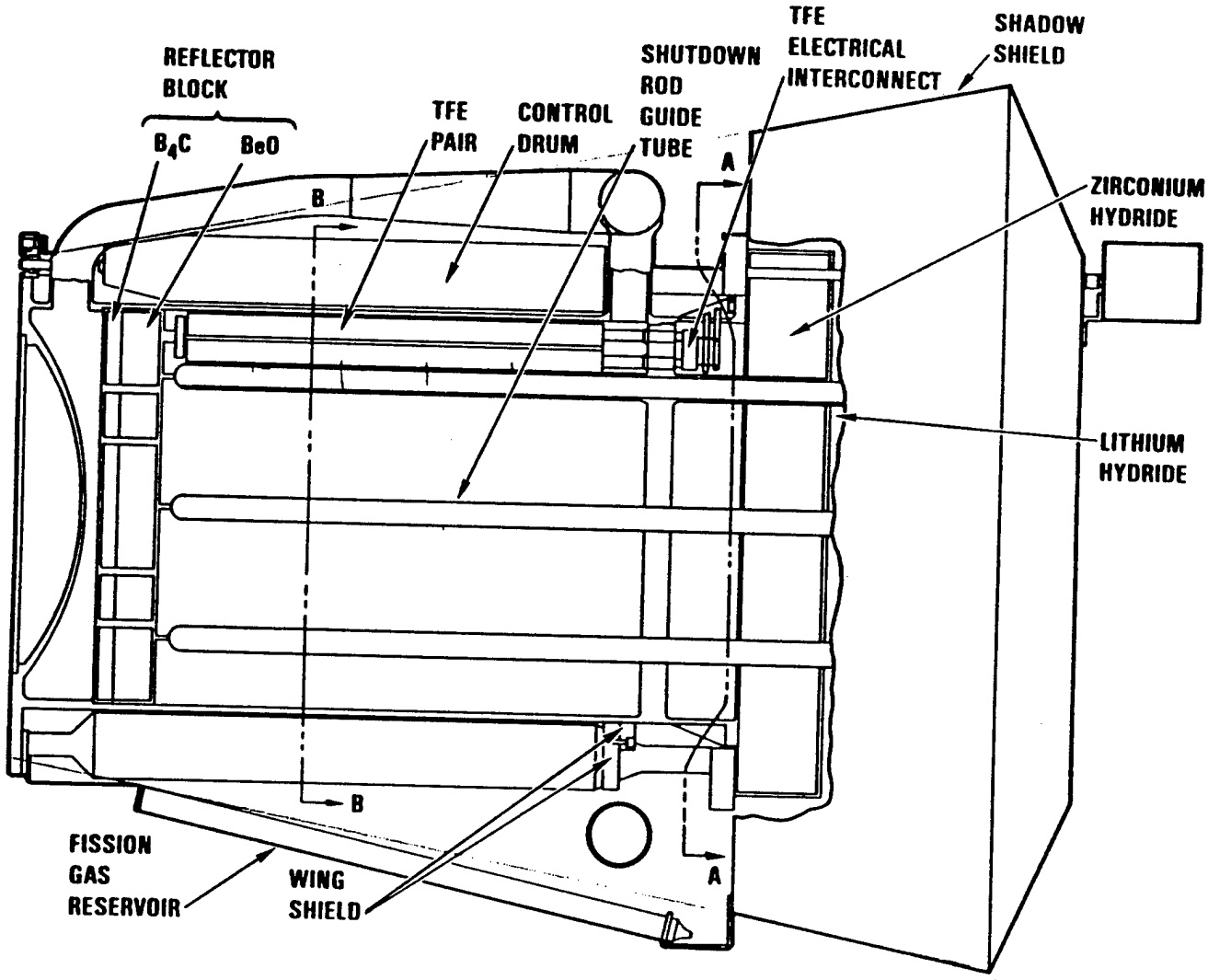

Figure 2.4: Schematic Diagram Of An All-TFE Space Reactor

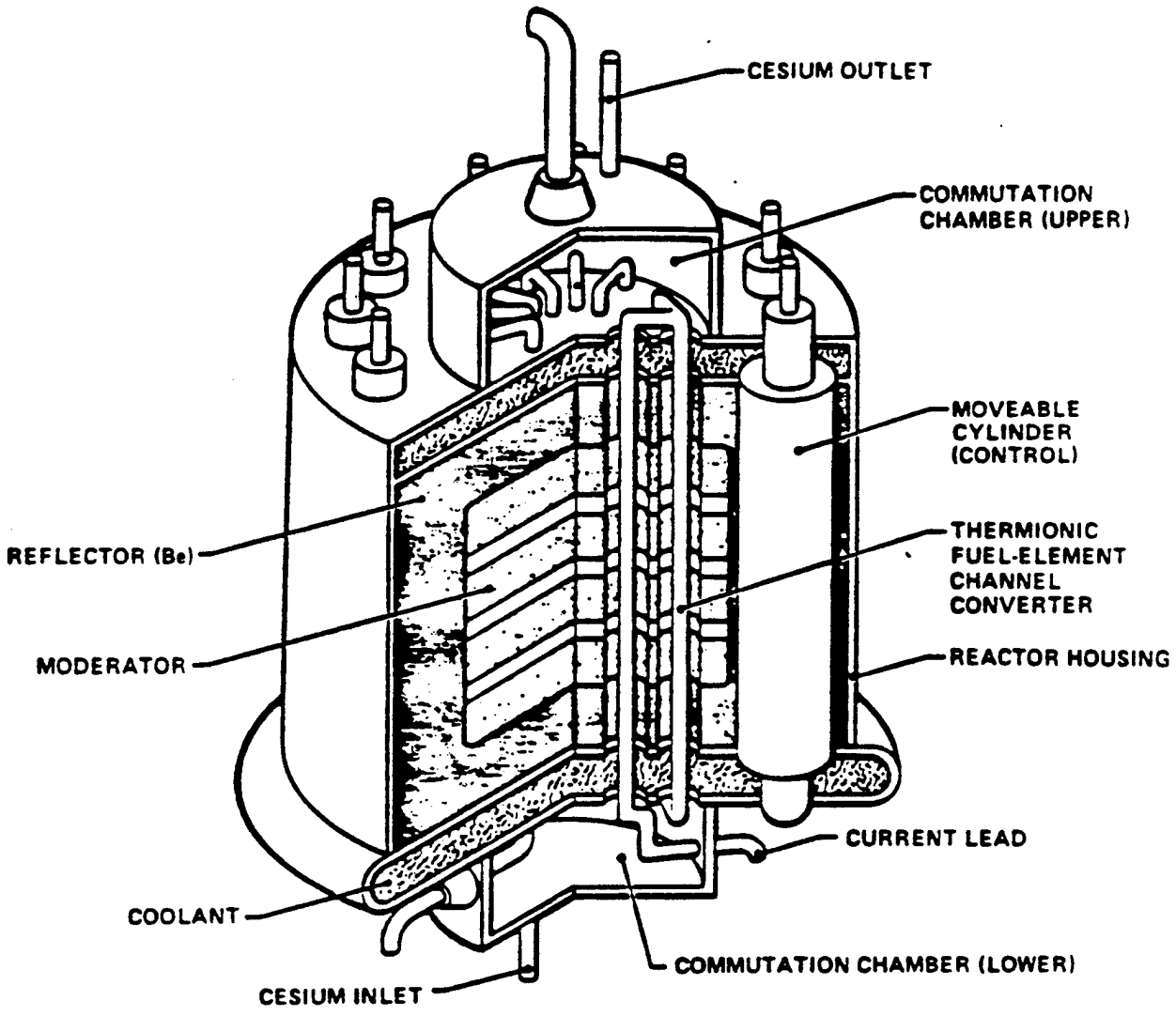

Figure 2.5: Schematic Diagram Of The "Topaz" Moderated TFE Space Reactor (Ref. 6).

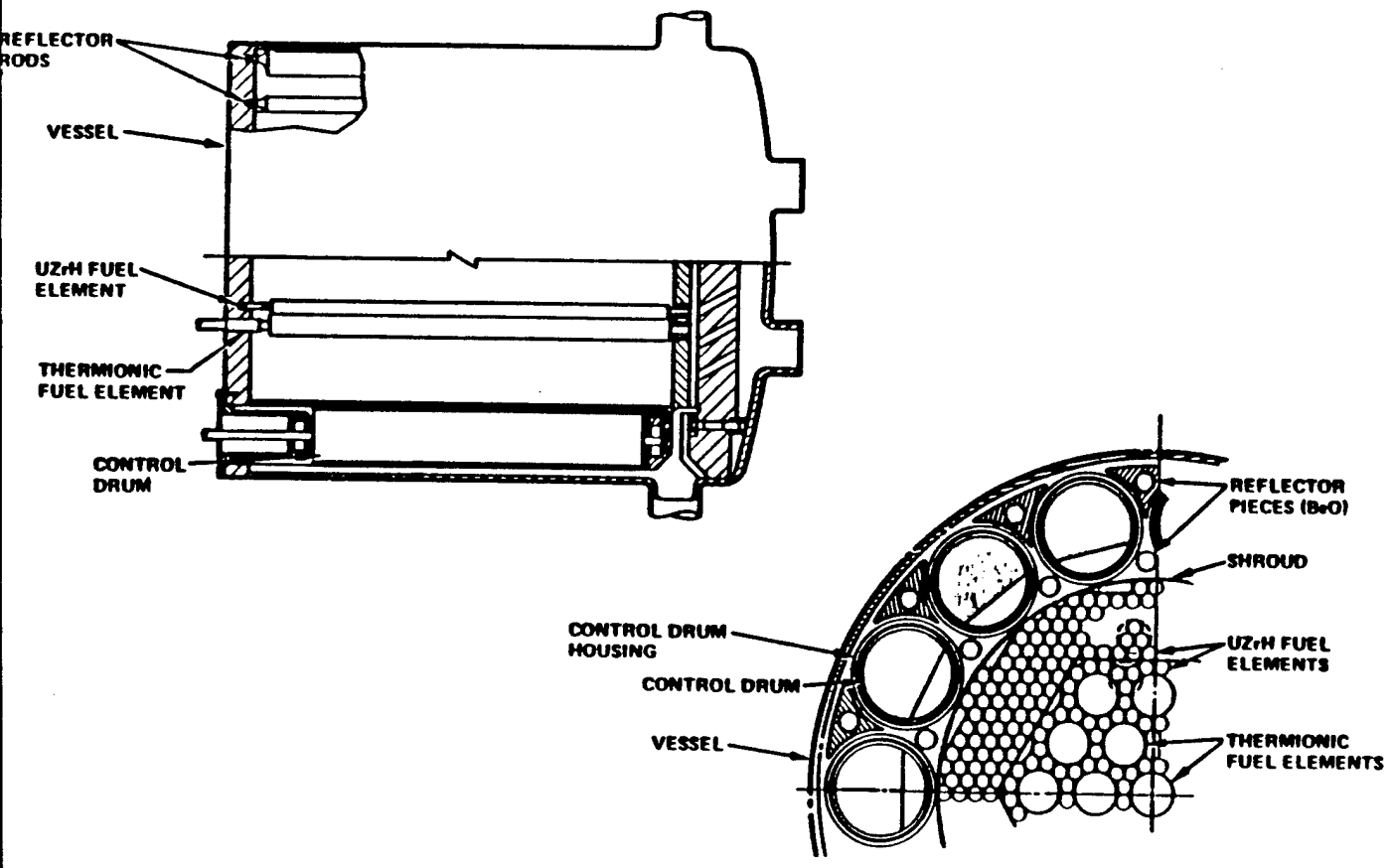

Figure 2.6: Schematic Diagram Of A Moderate TFE Reactor With Driver Fuel (Ref. 6).

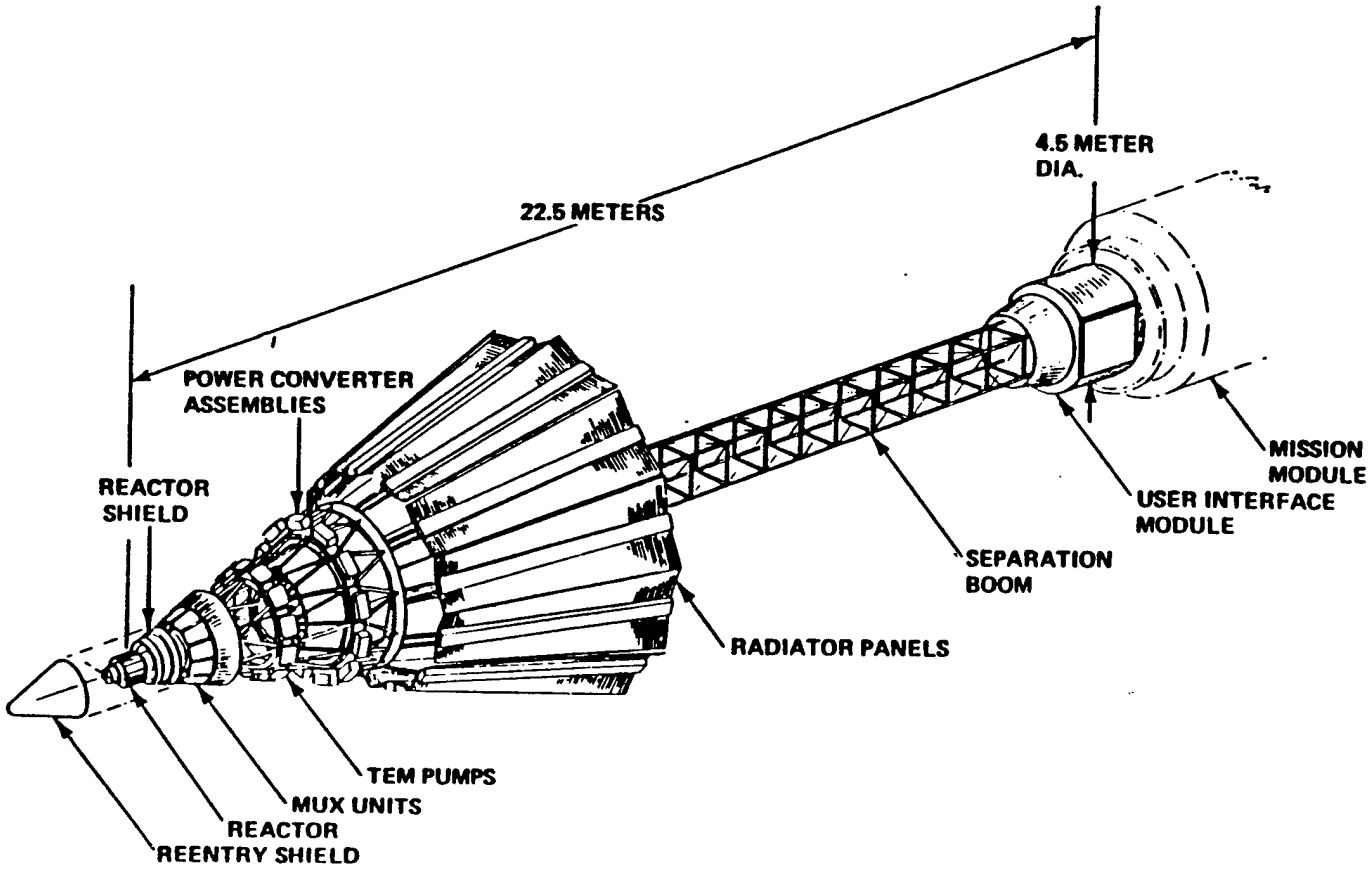

Figure 2.7: Schematic Diagram Of The SP-100 Thermoelectric Space Power System (Ref. 7).

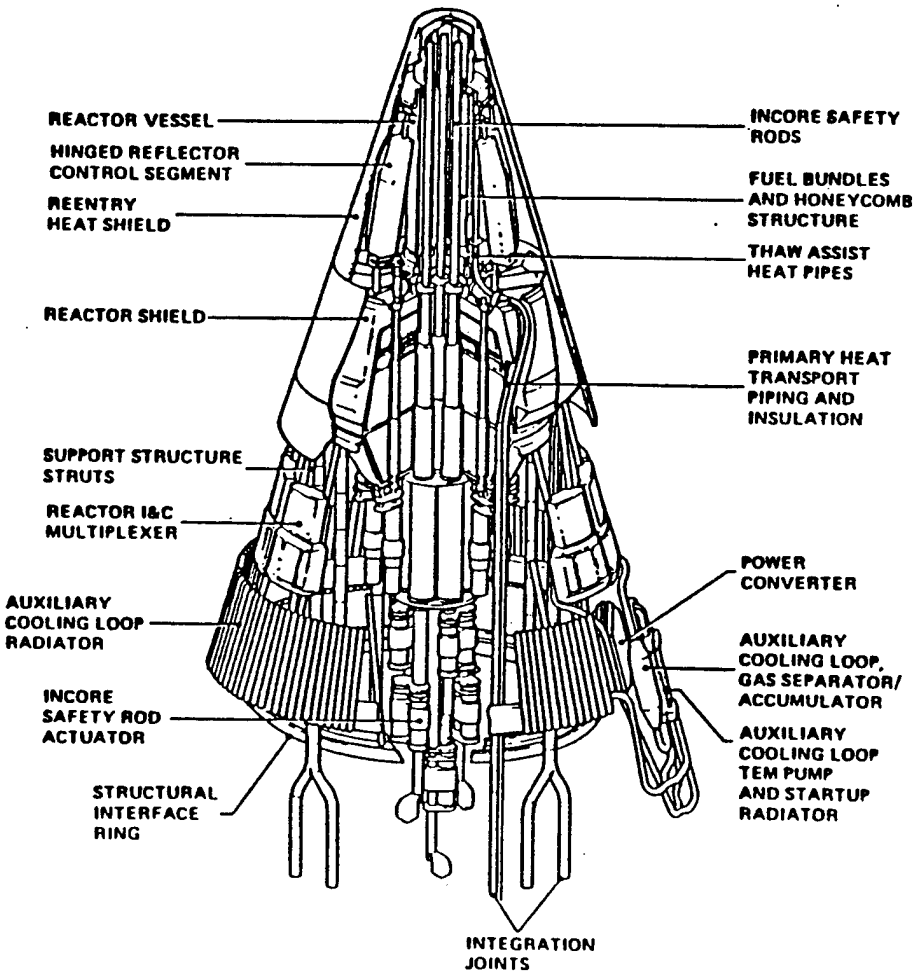

Figure 2.8: Schematic Diagram Of The SP-100 Primary Coolant Loop (Ref. 7).

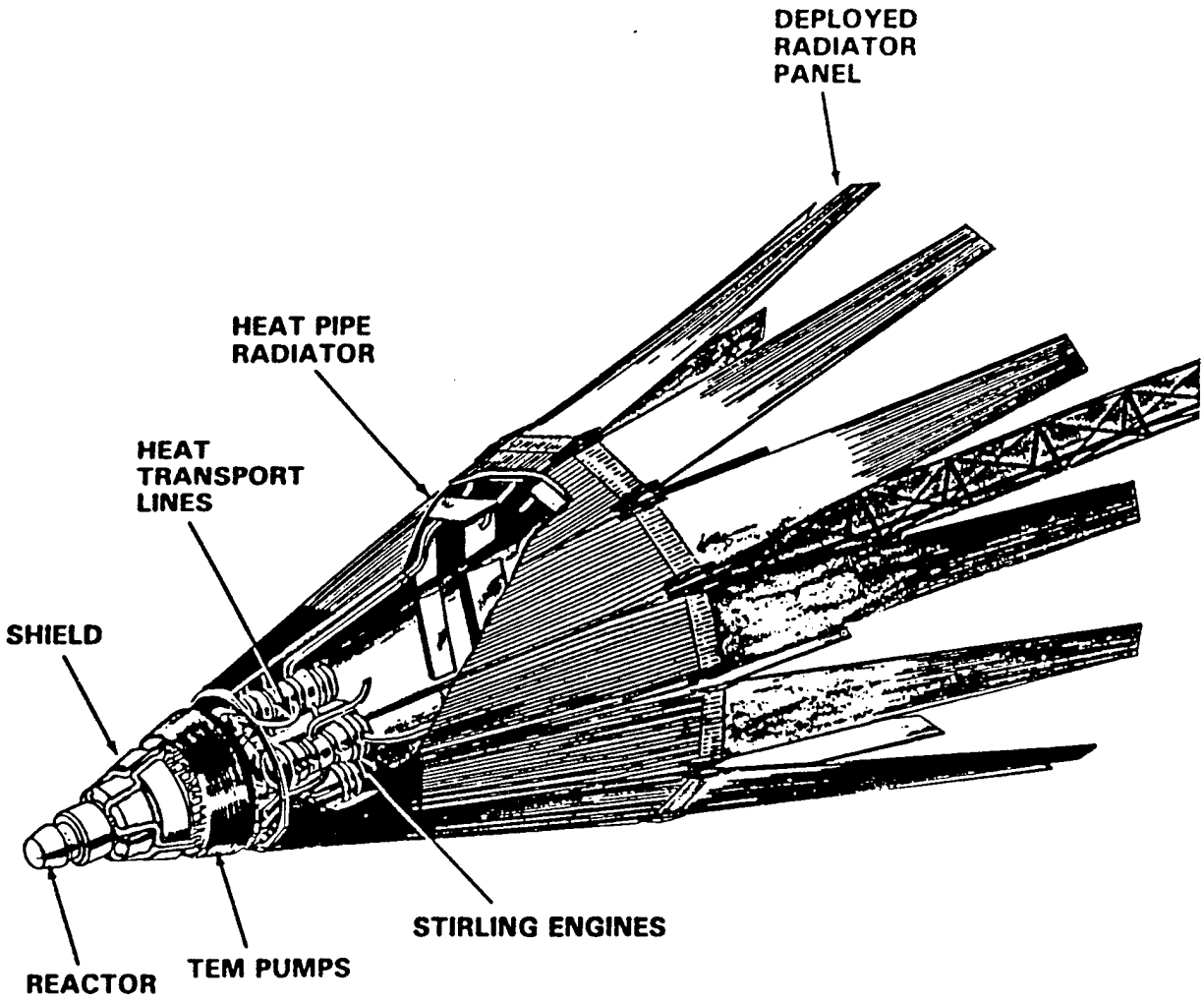

Figure 2.9: Schematic Diagram Of NASA's SP-100/Stirling Power System

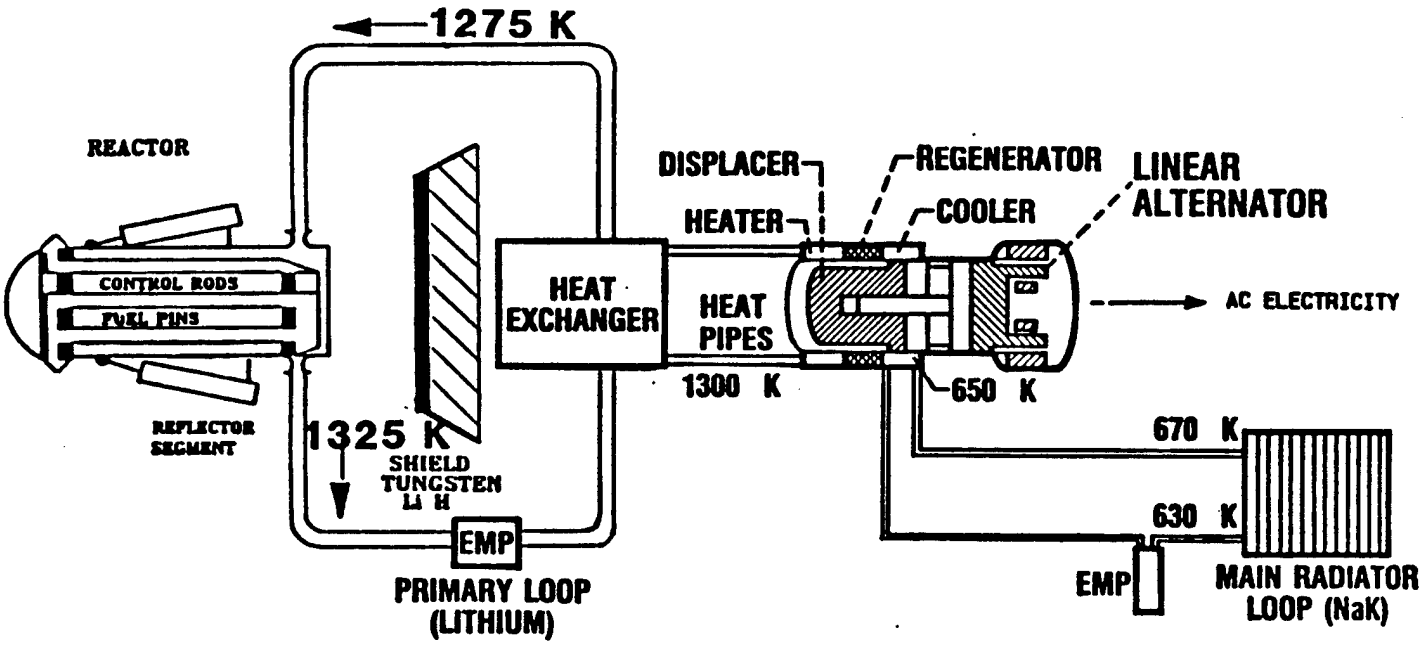

Figure 2.10: Flow Diagram Of NASA's SP-100/Stirling Power System

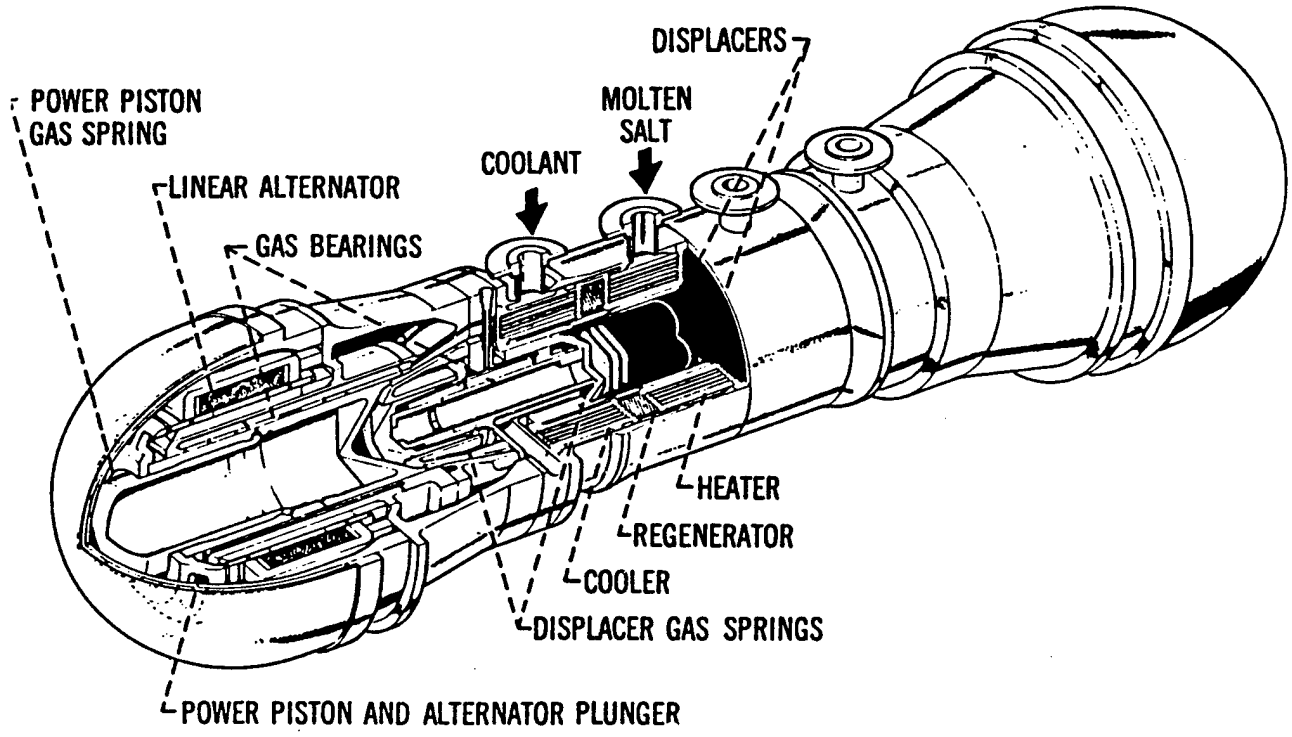

Figure 2.11: Schematic Diagram Of A Stirling Engine

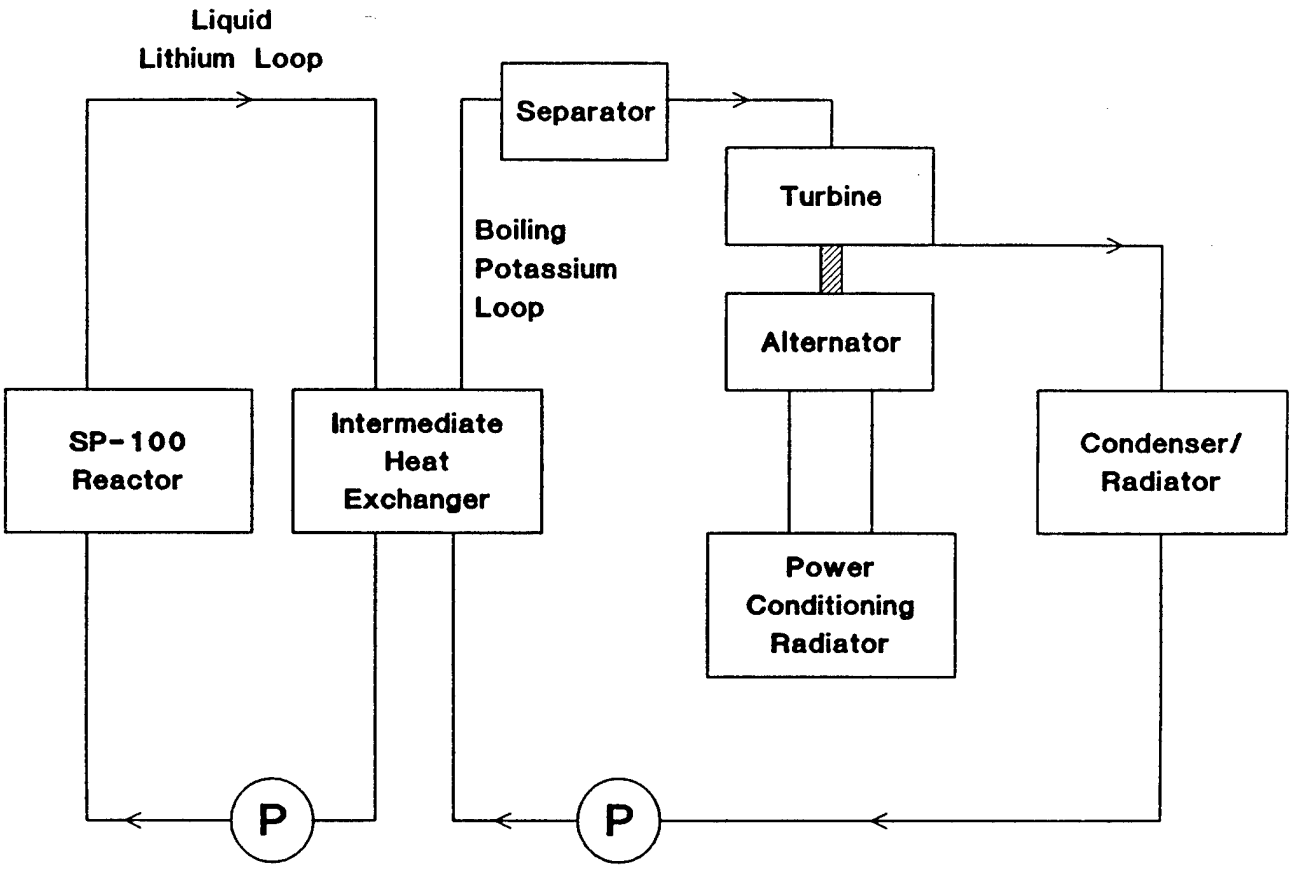

Schematic of the SP-100 Rankine Concept

Figure 2.12: Flow Diagram Of The SP-100/Rankine Power System

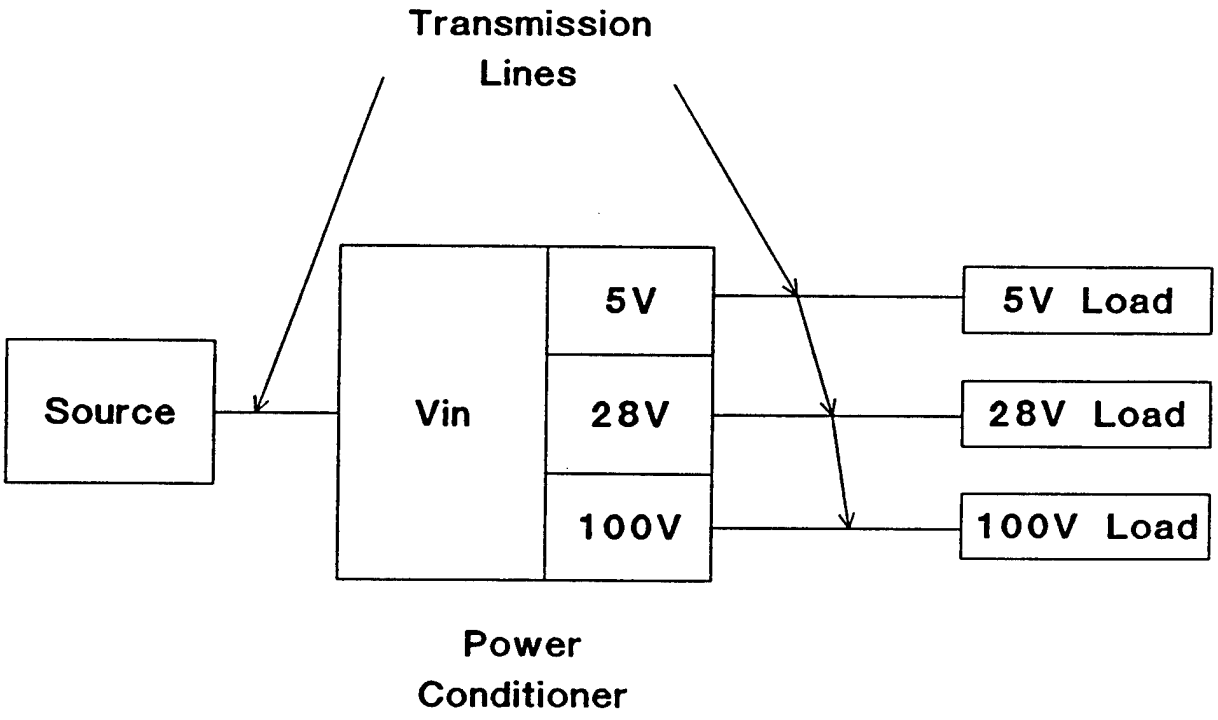

Figure 2.13: Simplified Electrical Flow Diagram

3.0 Analysis Approach

In any comparative systems analysis it is absolutely essential to pick a common set of ground rules against which to assess the various concepts. When time and resources are limited, as in this case, these ground rules must be simplified to the point that they address only major issues. As a result, we have performed top level system mass, area, and performance analyses and presented results as part of the general discussion. We have optimized component performance within the constraint of minimizing overall power system mass for all of the more massive components, intentionally omitting many minor components which when added together may make real system masses different than the estimates shown here. However, special care was taken to treat the SP-100 thermoelectric concept in identical fashion to the other concepts since it has received more design funding and has therefore identified many additional contributors to total system mass. We did not permit major concept re-design in our optimization process but only varied component parameters within the range permitted by each design. Because of the simplifying assumptions, our results will not be completely representative of real systems nor are they intended to be because many design details are unknown at this time. They should however provide good relative comparisons among the various concepts. We believe our approach is reasonable because our results agree well with those obtained from the SP-100 program for the SP-100 thermoelectric and innovative SP-100 concepts.

The remainder of this chapter describes the approach that was used in our analyses to obtain consistent mass and area estimates among the various power system options.

3.1 Description of System Models

The mass and area estimates presented in this paper were derived from models developed at Sandia. The objective of these models was to develop a consistent set of estimates based on design approximations and to a lesser extent on known component masses. For example, design approximations are used to determine reactor fuel mass. The fuel masses required to meet criticality limits, fuel damage limits, burn-up limits, thermal limits, etc. are calculated and the fuel mass selected is the largest of these cases (Ref. 11, 12, 13, 14, 15, 16). The mass of the radiation shield for the power conditioning system is also based on design approximations but power conditioning mass and volume are estimated from known component values (Ref. 10). The level of detail in each of the models is consistent and some of the subsystem models used in the various system models are

the same. As a result, we believe the relative comparison between the various power systems is quite good. Furthermore, the SP-100 program's own detailed mass estimates indicate that our absolute values should be reasonably representative of actual mass.

Another important characteristic of the models developed for each system is that all of the subsystems are contained in one model. Therefore, the interactions between the various subsystems is modeled. For example, the thermal power required from the reactor is not known until the efficiency of the electrical system is known. This is further complicated by the fact that each component of the electrical system cannot be designed until the efficiency of the other electrical components is known. By having all of the subsystem models contained within a single model, these interactions are taken into account.

The final, major characteristic of the models is that the mass of the power systems can be optimized at each power level. The optimization is based on the important system parameters. In the OTR concept, for example, the amount of power obtained is directly proportional to the surface area of the reactor core. Therefore, the model varies the height to diameter ratio of the core as specified by the user. The system mass is calculated for as many ratios as desired and the code selects the optimum ratio based on minimum total power system mass.

The differences between military and civilian programs are not reflected in our calculations, because we did not require the power systems to survive hostile threats that could be postulated for military missions. The mass and area estimates are therefore applicable to either civilian or military missions at the selected orbit altitude.

3.2 Study Ground Rules

The specific ground rules for this study are shown in Table 3.1 and are discussed in detail below.

3.2.1 Technology Status

Perhaps the most significant ground rule and the one most often neglected in many conceptual proposals requires us to consider only near-term or nearer technology in our conceptual system estimates. This has far reaching implications. For example, we believe that power conditioning devices can be developed that will tolerate higher radiation doses and operating temperatures than

presently possible; but not in the near-term. This means that the reactor shield and the power conditioning radiator will be heavier in a near-term system than one built later using power conditioning devices which could operate in higher temperature and radiation environments.
There are of course many different opinions regarding what is and is not "near-term" technology and our opinion is only one of a very large set. We have used the following general definition for "near-term" technology:

> "We expect that necessary parts and materials could be developed and a prototype proven by hardware testing on the ground within 5 years if a concerted effort is made and funding is available to do so."

It is also important to recognize that technology risks and development costs are not the same among the systems labeled as near-term. For example, the SP-100 Thermoelectric Program has been under way since 1983 although the thermoelectric energy conversion devices employed in SP-100 have not yet been tested. A test program is in place which is successfully addressing the technical issues associated with thermionic fuel element energy conversion devices and STAR-C utilizes a flat plate thermionic diode conversion approach that has been under development for years. Nonetheless, the Thermionic Fuel Element and STAR-C concepts are based primarily on studies and the fuel form STAR-C proposes has never been produced in the United States. None of the systems have demonstrated the ability of either the reactor or energy conversion systems to operate in an unattended mode for up to ten years. Free piston Stirling engines with linear alternators must overcome problems associated with wear, creep, and material degradation over the long system lifetimes at high temperature. The flat thermionic diodes used in STAR-C, the thermoelectrics used in SP-100, and the thermionic fuel pin devices must overcome problems of long term material degradation at high operating temperatures. Brayton turbines using helium-xenon as a working fluid have not been used to any great extent but one has been built by Garrett (Ref. 17) and it is reasonable to expect that this is the most mature conversion technology.

With two exceptions, the SP-100 reactor technology when it is coupled with liquid metal Rankine or refractory metal Stirling energy conversion systems, we have analyzed near-term concepts which we believe offer the greatest potential for small mass and radiator area. The exceptions were included to show the potential benefit of pursuing the two different conversion technologies for future systems. In both cases we assumed the use of advanced conversion technology while retaining the use of near-term technology

for the remainder of the system (i. e. SP-100 reactor technology, control electronics, etc.). The Rankine conversion technology is further out in time because it requires two-phase flow in a micro-gravity environment and turbines and vapor separators must be developed and proven reliable for long term use with liquid metals at high temperatures. These are issues that will not be resolved for several years. The free piston Stirling engine must use refractory metals at the hot end in place of superalloys if it is to operate at 1350K as we assumed in one of our system analyses. The superalloy version of this engine is currently under development at NASA's Lewis Research Center and should be available in the near-term. The refractory metal engine would result in a lighter system but it would not be available in the near-term if the present evolutionary approach being pursued by NASA is continued (Ref. 18). In this approach, a superalloy engine is being developed for initial testing up to 1050K. It is being designed in such a way that, once the design is proven, refractory metals could hopefully be substituted for superalloys in certain components without redesign. Then a refractory metal engine could be put on test. This requires that test facilities be upgraded to provide a vacuum of 10 to the minus 7 to 10 to the minus 8 torr, and that materials fabrication and joining processes be developed. If their were sufficient demand for a refractory Stirling engine, a revolutionary approach to go directly to that engine could conceivably develop one in the near-term but at much higher development risk. For these reasons, we conclude that superalloy Stirling engines are near-term and refractory engines are far-term.

3.2.2 Reliability

In a top-level systems study such as this, with most of the concepts in very preliminary form, it is not possible to adequately treat the effect of required reliability and therefore component redundancy on system mass. No system reliability analyses were done. However, we have included cursory estimates where possible by arbitrarily assuming that the probability of producing 100% of the design power level after 10 years should be 95%. Of the 5% unreliability, 2.5% was assigned to degradation of the various heat rejection radiators due to micrometeoroid damage to heat pipes and the other 2.5% to the balance of the system. Thus, since there would be a large number of heat pipes whose failure would only reduce system power incrementally, there is a 97.5% probability of the system producing a significant percentage of system power after 10 years. We assumed 10% redundancy in the power conditioning subsystem and 20% for the transmission lines. In the case of turboalternators and Stirling conversion systems we assumed 20% redundancy, which means these

systems would use six conversion units with five operating and one in the standby mode. Using a large number of conversion units may or may not practical, but the assumption is adequate for mass estimation purposes. In the turboalternator case, the spare engine would probably be running but producing no power in the standby mode to counter-balance torques generated during turbine start-up and any other operations that require changes in speed.

3.2.3 Component Mass Estimates

Our power system mass estimates include the reactor, shield, power conversion, power conditioning, power transmission, heat exchanger, and radiator subsystems plus the structure required to interface with the user satellite but not the satellite itself. Area estimates include radiators to dump the waste heat from reactor and power conversion equipment, power conditioning and transmission equipment, and reactor control electronics but do not include a satellite electronics radiator.

The mass estimates for the reactors were obtained based on the following considerations. The structural mass associated with the reactor such as cladding and TFE internal structure is explicitly included. In addition a number of miscellaneous structural components such as reflector supports, fittings, springs, etc. are included by multiplying the core volume by a core-average miscellaneous structural density that was obtained by dividing the miscellaneous structural mass for the SP-100 100 kWe reactor core by its volume. Safety system mass estimates are based on the assumption that all reactors will require a redundant reactivity control safety system plus a re-entry aeroshell. The reactor core volumes are arbitrarily increased by 20% to account for the in-core redundant reactivity control system unless they already have enough space for this system. The mass of the redundant reactivity control system is then estimated for all concepts by multiplying the resultant core radius by a number obtained by dividing the redundant reactivity control system mass for the SP-100 100 kWe design by its core radius. The mass of the re-entry aeroshell is taken from the SP-100 program and scaled to other systems based on reactor geometry. In addition to these two safety system components, all concepts except the OTRs include an auxiliary coolant loop to prevent meltdown in case of a loss of coolant accident. The mass of a rhenium barrier is also included to provide negative reactivity for core flooding accidents in all concepts except the OTRs. The OTRs are excluded because their tungsten emitter could concievably be replaced with a rhenium emitter that would meet this requirement. The instrumentation and control mass is broken down into three components: 1) fixed items

that change very little with power level or reactor size, e.g., controllers and multiplexers, 2) size dependant items that increase appreciably with power level or reactor size, e.g., control and safety drives and actuators, and 3) items dependent on boom length, e.g., I&C cabling. The mass densities and linear densities for these components were obtained from the SP-100 100 kWe reference design. (Note: Since OTRs do not have to control an active coolant loop the components used for that function were omitted from the OTR estimates.)

Mass estimates for all of the radiators include armor to protect them against micro-meteoroids. We assume that armoring is provided by simply increasing the thickness of the heat pipe radiator walls since these are near-term systems. If graphite armor were available, the associated mass could be reduced. The armor is thick enough that the radiators have a 97.5% probability of being fully operational after ten years operation at the selected orbit altitude. Any penetration of the armor would cause only limited degradation due to redundancy of the heat pipes in each radiator. The specific masses used for the waste heat radiators are 6.8 kg/m^2 for temperatures below 690K and 8.2 kg/m^2 for temperatures above 690K. Micro-meteoroid protection was not included for any other components since we lack both the design detail and the time to do so. It is of interest to note that space debris is not yet a threat at the selected orbit altitude which is fortunate because it is impossible to protect against space debris without huge mass penalties.

Mass estimates also include aluminum shielding around all electronics of sufficient thickness to limit the dose from protons and electrons in the Van Allen belt to 20% of the total dose that the electronics must survive.

Mass estimates for the radiation shields consider:

reactor control electronics which operate at 300K and can withstand 10^{16} neutrons/cm^2 and 0.5 Mrad of gamma radiation

power conditioning electronics which operate at 425K and can withstand 10^{13} neutrons/cm^2 and 1 Mrad of gamma radiation.

satellite payload devices which operate at 300K and can withstand 10^{13} neutrons/cm^2 and 1 Mrad of gamma radiation. Since the power conditioning electronics are limited to 10^{13} neutrons/cm^2, the payload need be no harder than that and we arbitrarily assume that all

payload electronics, sensors, and other functions can meet or be locally shielded to survive the above payload environment.

that all components are shielded so that no more than 80% of the above specified doses comes from the reactor and no more than 20% from the natural environment.

a varying separation distance between the reactor and the satellite payload optimized to minimize total system mass (See Figure 4.4 for a typical example).

Boom mass is assumed to be 9 kg/meter which is typical of the berylium design proposed for the SP-100 thermoelectric system. We calculate that such 20 m boom cantilevered horizontally could support a 1100 kg load at 1 g without exceeding yield stresses in the materials. This assumes that the joints of the fully extended boom could be made as strong as the parent material. Such a boom would permit significant g-loading during maneuvers to avoid hostile threats if necessary.

TABLE 3.1: GROUND RULES FOR MASS AND AREA ESTIMATES

Application:	General civilian or military satellites
Technology:	Near-term
Mission Duration:	10 years
Power:	Variable from 5 to 1000 kWe
Payload Voltage Requirements:	
	15 % at 5 volts dc 55 % at 28 volts dc 30 % at 100 volts dc
Electronics Hardness:	0.5 Mrad gammas and 10^{13} neutrons/cm^2
Orbit:	Circular, 3000 km, 90 degree inclination
Durability:	Must endure natural and reactor induced environments - micro-meteoroids, Van Allen belts, cosmic and reactor induced radiation
Survivability:	Hostile military threats not considered

4.0 Mass and Area Results

4.1 Power System Mass Comparison

The estimated masses of the 9 reactor power systems we investigated are shown in Figures 4.1 and 4.2 as a function of power level. Figure 4.3 is a plot of specific mass versus power level. It is worth reiterating that the absolute values shown for mass are our best estimates, and we have not yet made a large effort to estimate the error associated with them. However, by looking at the SP-100 thermoelectric system mass at 100 kWe, it can be seen that our estimate is about ???% higher than the estimate currently being made by the SP-100 program (Ref. 7). Our estimates for the 10 kWe innovative SP-100 are 7% lower than the DOE estimate (Ref. 19). Also, although we believe the best use for the mass curves is for relative comparisons, they should not be interpreted too literally. Single curves depicting these results can be misleading unless broader issues are considered. For example, our estimates show the cross-over between the STAR-C and SP-100 thermoelectric concepts to occur at 22 kWe. However, from separate sensitivity analyses we know that with the uncertainties in actual performance the masses of STAR C and SP-100 thermoelectric systems could occur anywhere between 15 and 30 kW(e). With these caveats in mind, the physical significance of the curves is described below.

4.1.1 OTR Power Systems

The slope of the STAR-C mass curve is steep throughout the power range of 5 to 50 kWe. The reason for this poor scalability is two-fold. First, the OTR concepts are fundamentally different from all of the other concepts. Above about 8 kWe, the size of the reactor core is set by the core surface area needed for heat transfer. Thus, the core size increases linearly with electrical power. Second, the STAR-C design is not optimized. The optimized OTR curve shows the potential that this design concept has to scale with power. The optimized OTR is the least massive system below about 25 kWe and is less massive than the SP-100 thermoelectric and innovative SP-100 at power levels below 50 kWe. (It should be noted, however, that the masses for the OTR above 30 kWe do not reflect problems with fitting the heat rejection radiator above the radiation shield. A minor mass penalty will probably be incurred when this is done.) A detailed discussion on the scalability of OTR power system can be found in Reference 3.

4.1.2 The SP-100 Power System.

Figures 4.1 to 4.3 have two curves representing the mass of the SP-100 power system. The more massive of the concepts is for a scaled version of the system being developed in the SP-100 program. The less massive is the innovative SP-100, which does not have a secondary coolant loop and only applies to power levels below about 30. The slope of both of the SP-100 systems is much steeper than the slopes of the other liquid metal cooled concepts. In fact, the slope is the same as that of the optimized OTR. The steep slope can be seen best in Figure 4.2. There are two reasons for the steep slope. The main reason is the low efficiency of the thermoelectric conversion system; the multicouple efficiency is 4.7% and the total system efficiency 4.2%. As a result, the masses of the reactor and heat rejection radiator both increase faster with increasing power requirement than for the other liquid metal reactor options. The second reason for the steep slope is that the specific mass (in kg/kWe) of the thermoelectric conversion units is high.

4.1.3 The SP-100 With Brayton Power Conversion

Aside from the potential reductions in mass of the STAR-C concept, probably the most interesting result obtained in our analyses is the excellent scalability of the SP-100 reactor used in conjunction with a Brayton power conversion system. It is the least massive of all of the near-term power systems at power levels above 25 kWe. In fact, it even scales better than the SP-100 with a refractory Stirling power conversion system, which is not a near-term system. The only power system that scales better is the SP-100/Rankine system. It is 14% lighter than the SP-100/Brayton system at 100 kWe and 34% lighter at 1000 kWe.

As was mentioned earlier, the gas-cooled reactor/Brayton power system was not analyzed in detail because of financial constraints; we did not have the time to develop the criticality model for the reactor. However, our mass estimate for this power system at 1000 kWe, which will not have a reactor that is criticality limited, is within 1% of the mass estimate of the SP-100/Brayton estimate.

4.1.4 TFE Based Power Systems

The TFE based power systems do not scale very well at the very low power levels. They are the most massive power system below about 22 kWe. However, as the power level increases, they become much more attractive. Above 85 kWe, they are lighter than all other near-term power systems except the SP-100/Brayton system. The reason for the poor

system performance at low power levels is that the reactor and shield are much more massive than for the other systems. The reactor is more massive, because it contains moderator and more structure and has larger dimensions. The shield is more massive, because it has a larger diameter, which is caused by a larger reactor. TFE based systems perform better at higher power levels for two reasons. First, they have a high temperature radiator (~1000K), which means that it will be smaller and less massive. Second, at the higher power levels, the power conversion systems of the dynamic systems contribute a substantially higher fraction of the total system mass than at lower power levels (See Section 4.2).

4.1.5 SP-100 With Stirling Power Conversion

Two SP-100/Stirling power systems are shown on Figures 4.1 to 4.3. The masses represented by the broken line is for a near-term, superalloy power conversion system, and the dotted line is for a future, refractory metal power conversion system. The near-term Stirling scales much better than the SP-100 thermoelectric system. It is 32% less massive at 100 kWe and 38% less massive at 1000 kWe. The refractory Stirling version scales better than the superalloy Stirling, mainly because it has a higher heat rejection temperature, and therefore, a smaller radiator. Although the efficiencies of the SP-100/Stirling systems are 3 to 6% higher than that of the SP-100/Brayton system, they are still more massive. This is due primarily to the fact that the Stirling engines themselves are so massive. At 1000 kWe, the superalloy engine is 40% of the total power system mass and the refractory engine is 50% of the total system mass. (Note: The Stirling engine mass algorithm was obtained from the NASA/Lewis Research Center.)

4.1.6 SP-100 With Rankine Power Conversion

The SP-100 with a Rankine power conversion system, which is not a near-term power system, scales better than any other power system above 25 kWe. The reasons for this are that it is a relatively high efficiency system with a small, high temperature, waste heat radiator and the Rankine turbo-alternator scales well with power level. At 300 kWe, it is less massive than the refractory Stirling and the Brayton systems by 40% and 24%, respectively.

4.2 Power System Mass Characteristics

During the course of our analyses we discovered several interesting characteristics of power system masses. Three of these characteristics are discussed below.

4.2.1 Length Of The Separation Boom

Figure 4.4 shows the relative mass of a 100 kWe SP-100 thermoelectric system as a function of boom length. Our calculations give a minimum system mass with a separation of 16 m. This is substantially shorter than the 22.5 m the SP-100 program uses. Also, if the separation distance is reduced to 9 m, the system mass increases by only 2.4%. This indicates that if shorter booms were required by the satellite payload that only a small mass penalty would have to be paid.

4.2.2 Power System Mass Breakdown

The mass breakdown for a power system varies significantly as the power level varies (Figure 4.5). At low power levels, the reactor and shield make up the majority of the mass. A substantial contribution is also made by the balance of system, i.e., instrumentation and control, safety systems, the electrical subsystem, and the boom. As the power level increases, the power conversion system and radiator become more important.

4.2.3 Rad-Hard Electronics

The radiation hardness of the electrical subsystem and payload electronics can have a significant impact on system mass. This is particularly true at lower power levels. If it is assumed that electronics that should be available in 1995 are used, the radiation shield only needs to be designed to reduce radiation levels to 100 Mrad and 10^{15} nvt (Ref. 20 and 21). These values compare to 0.5 Mrad and 10^{13} nvt, which are used in this report. Figure 4.6 shows how the mass of an optimized OTR is reduced with these advanced electronics. At 10 kWe the mass decreases by 26%, and at 30 kWe it decreases by 21%. At the same time, the length of the separation boom for the 30 kWe system decreases by more than a factor of two.

4.3 Power System Area Results

A comparison of the specific areas of the heat rejection radiators for each of the power systems as well as the power conditioning radiators is given in Figure 4.7. The specific areas are for the power system beginning of life (BOL), i.e., they include an additional 10% area to account for heat pipe redundancy. It should be noted that the power systems were optimized based on total power system mass. Therefore, the radiator areas shown here could be reduced at the expense of mass, i.e., by using higher heat rejection temperatures and less efficient energy conversion.

The largest radiator belongs to the SP-100 thermoelectric power systems. This is due in large part to the fact that the system efficiency is 4.2%, which is very low compared to the other systems, and so almost 96% of the power generated in the reactor must be rejected. The next largest radiator is for the SP-100 with a near-term Stirling power conversion system. Its large size is due to the fact that it operates at relatively low temperatures: between 490 and 540K.

The third largest radiator belongs to the SP-100/Brayton power system. Its large size is also due to the fact that it has a relatively low temperature. The 20% change in the specific mass between 30 and 50 kWe is due to an increase in the effective radiator temperature. The temperature goes from a range of 379 to 843K to a range of 428 to 846K. This increase in temperature reduces the system efficiency from 24.8% to 22.9%, but reduces overall system mass. It should be mentioned that the specific area of the radiator drops again for the 1000 kWe SP-100 Brayton system. The drop results from an increase in the effective radiator temperature; the temperature range becomes 476 to 843K. This temperature increase is accompanied by a decrease in system efficiency to 20.2%.

The radiator specific area for the SP-100 with a refractory Stirling power conversion system is 0.42 m^2/kWe for all power systems above 20 kWe. This power system has a much smaller radiator than the SP-100/
superalloy Stirling mainly because of its higher temperature. The radiator temperature range is 590 to 640K, which is 100K higher than the range of the superalloy version.

The shape of the specific area curve for TFE based power systems is driven by the technologies involved. The 5 kWe system has both moderator, which forces the coolant temperature to be held at or below 900K, and driver fuel. Thus, it has a very low thermal efficiency, 2.1%, and a relatively low radiator temperature range, 840 to 890K. Between 10 and 50 kWe, driver fuel is no longer used, and so the thermal efficiency increases to 8.3%. Above 100 kWe, the moderator is no longer required and so the primary coolant temperature, and therefore the radiator temperature can be raised. In our calculations the temperature range increases to 990 to 1040K.

The specific areas of the STAR-C and OTR power systems are the next to smallest of all power systems investigated in this report. The small size is a result of good efficiency, 12 to 13%, and a high heat rejection temperature, 1000K. The system with the smallest specific area for the heat rejection radiator is the SP-100/Rankine

system. The small size is achieved through a high efficiency, 22%, and a relatively high heat rejection temperature, 900K.

The specific areas for the power conditioning radiators were based on a radiator temperature of 425K. The difference between the areas of the ac and dc power conditioning curves result from the fact that they have different efficiencies: 91% for dc and 96% for dc.

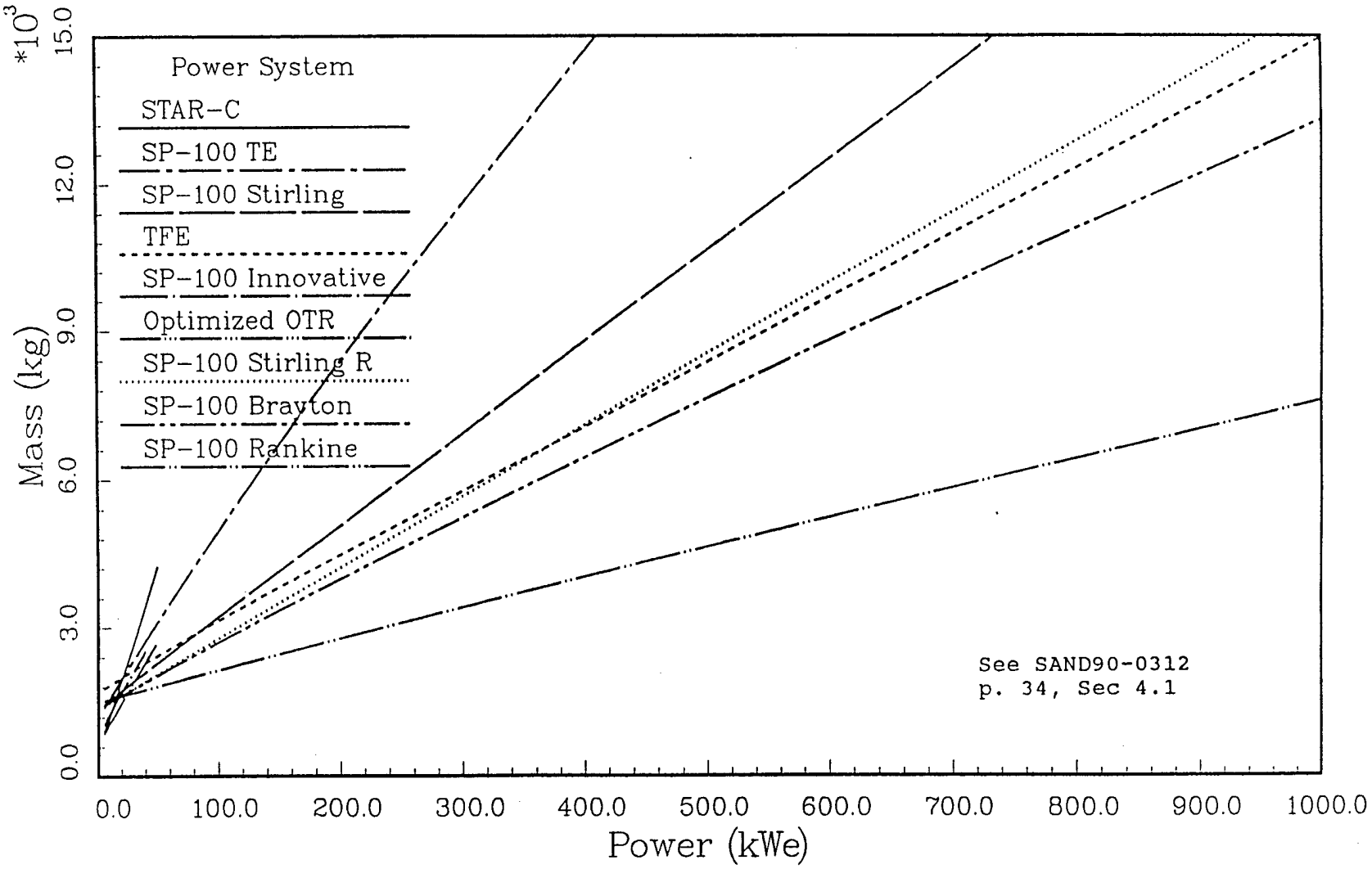

Figure 4.1: Scalability Of Space Nuclear Power Systems From 5 To 1000 kWe

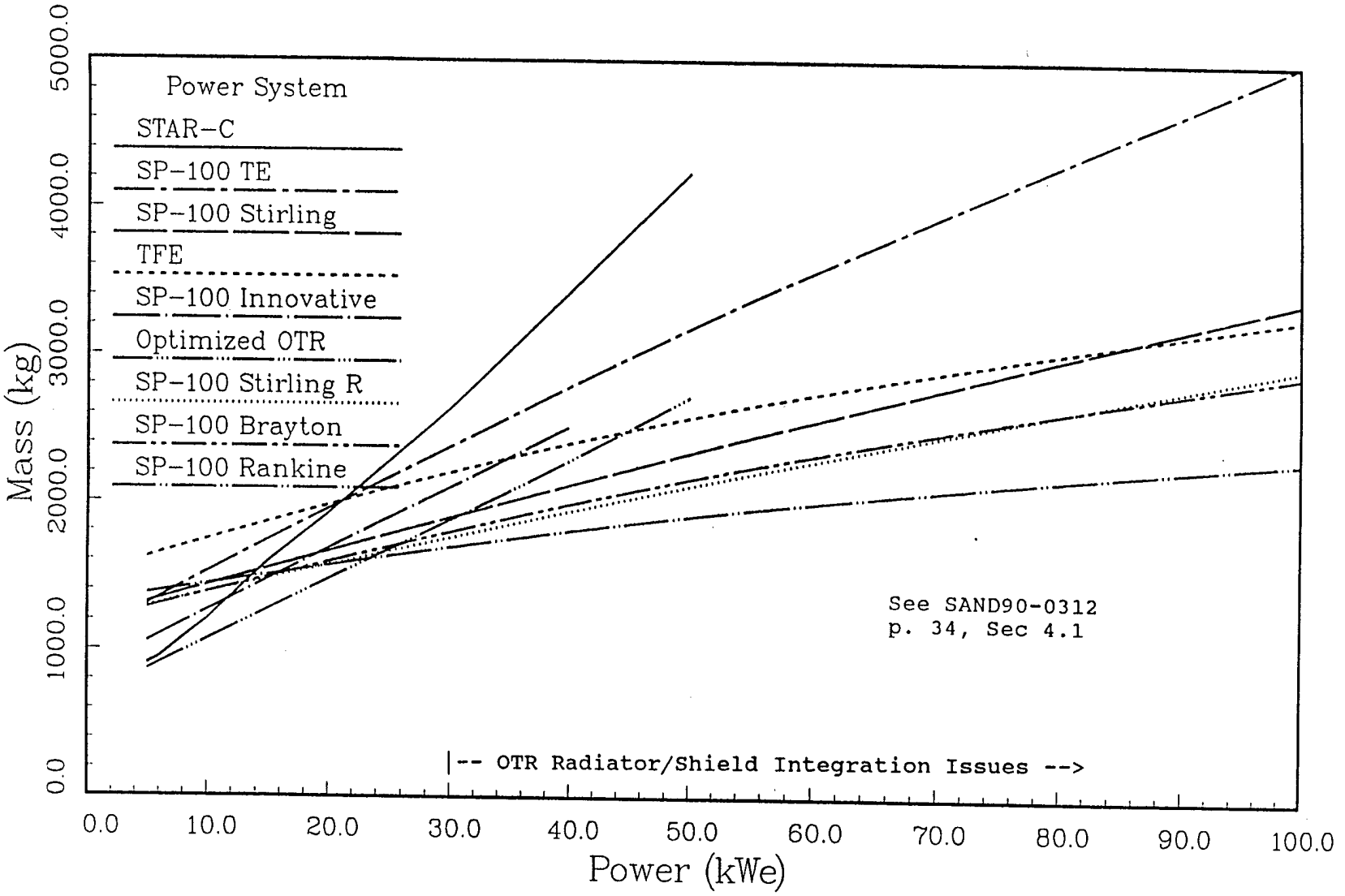

Figure 4.2: Scalability Of Space Nuclear Power Systems From 5 to 100 kWe

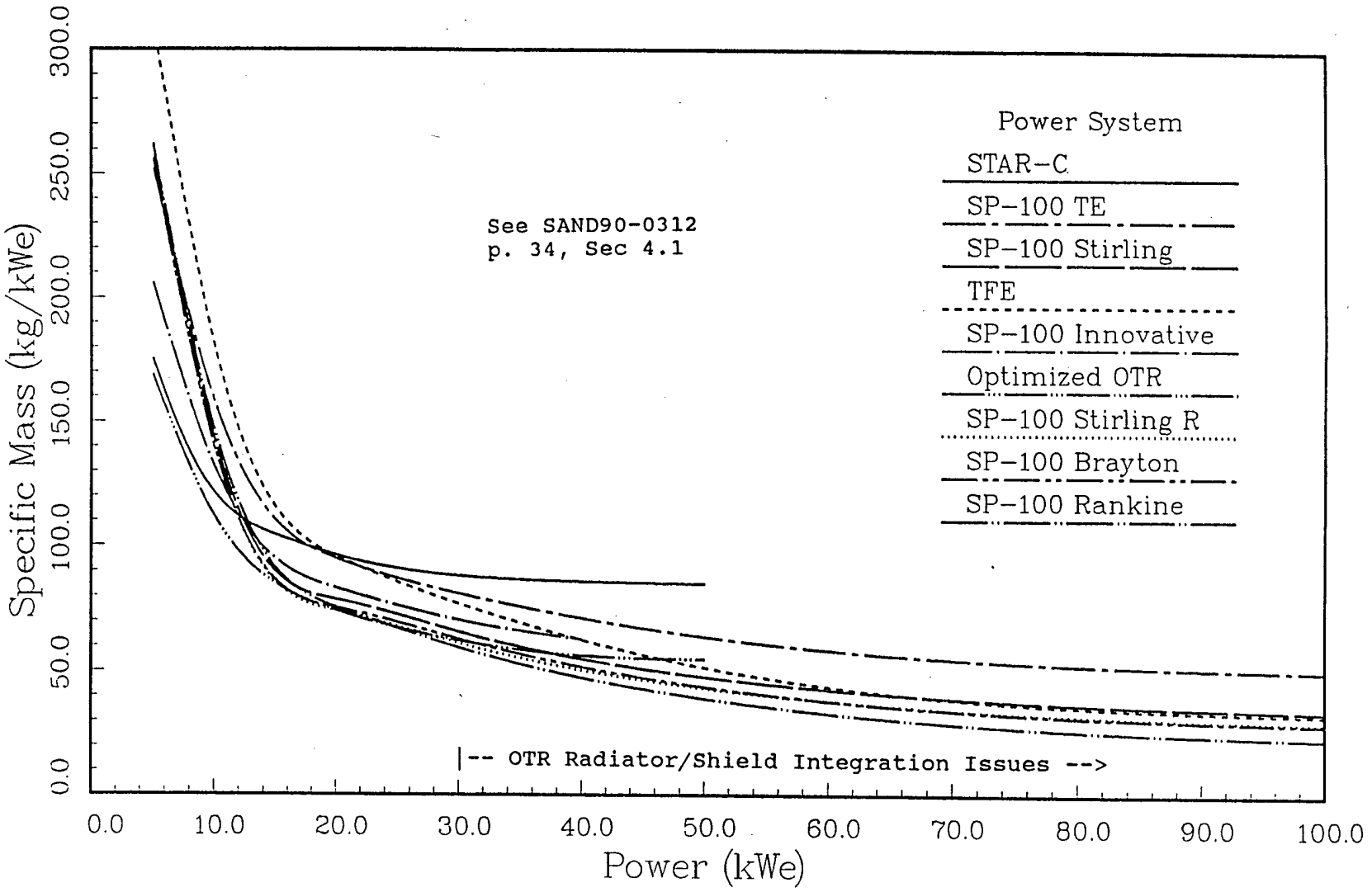

Figure 4.3: Specific Mass Of Space Nuclear Power Systems

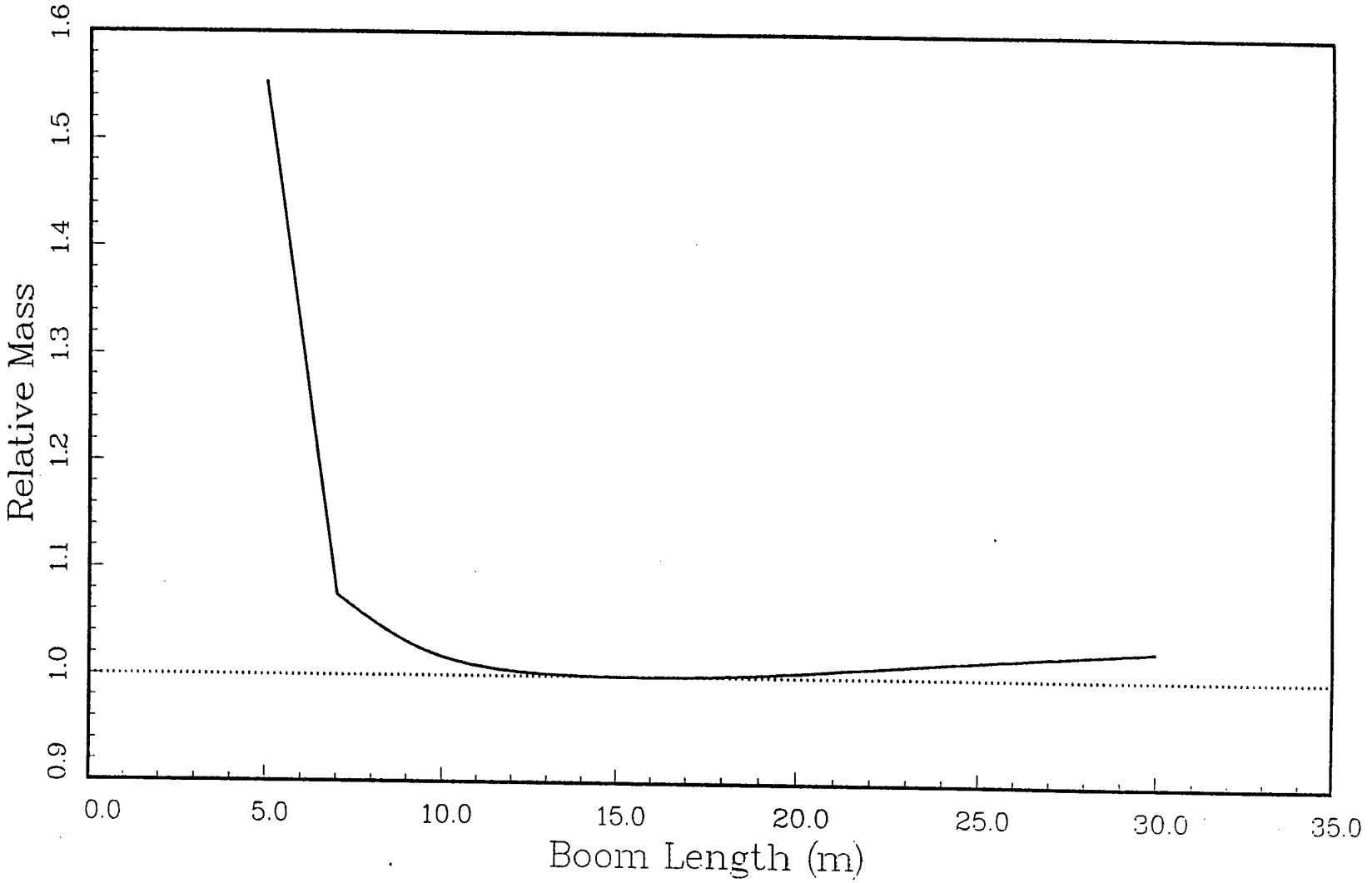

Figure 4.4: Relative Masses Of The 100 kWe SP-100 Power System As A Function Of Boom Length

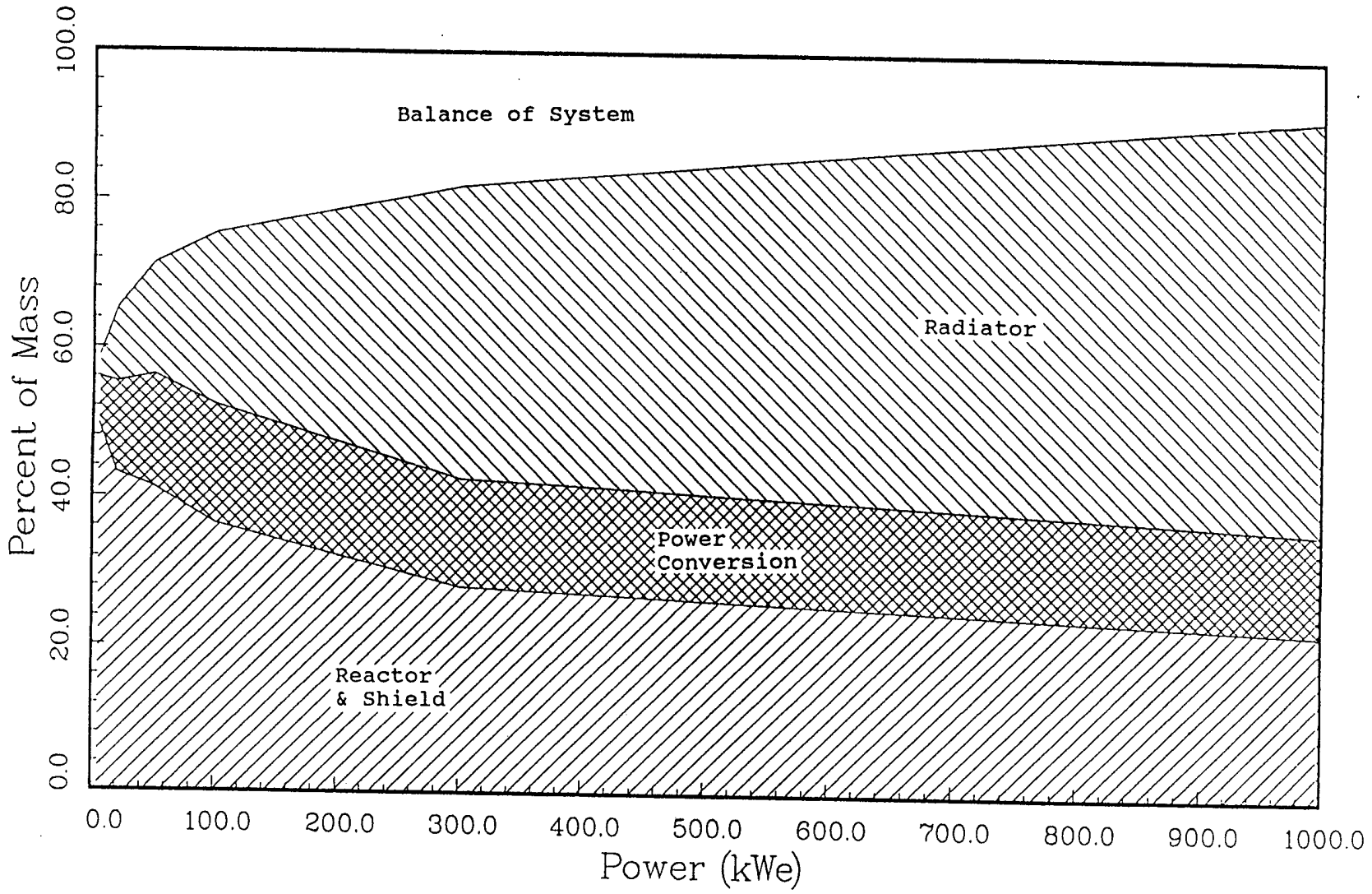

Figure 4.5: Mass Breakdown Of The SP-100/Brayton Power System As A Function Of Power Level

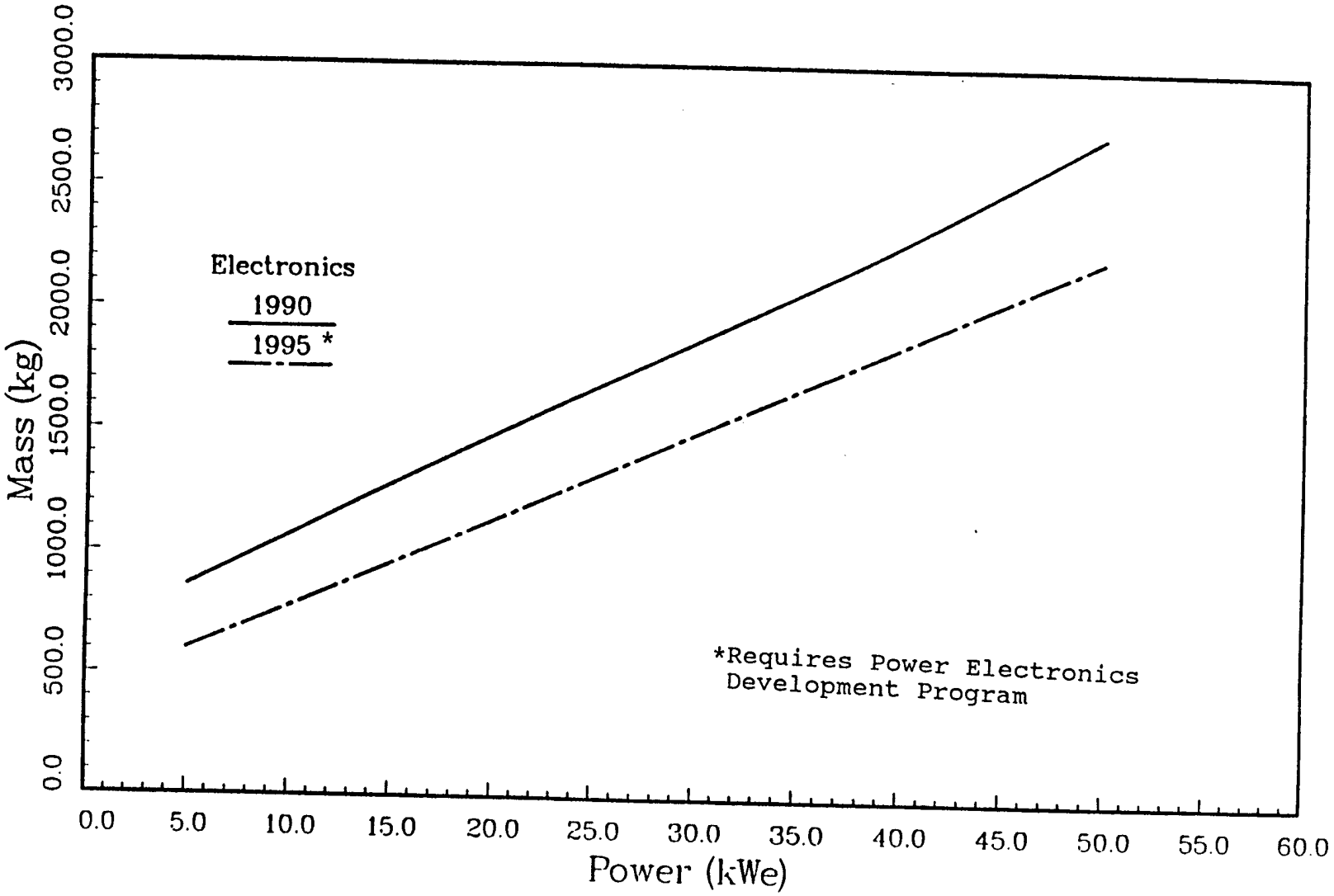

Figure 4.6: Impact Of Improved Rad-Hard Electronics On The Scalability Of An OTR Power System

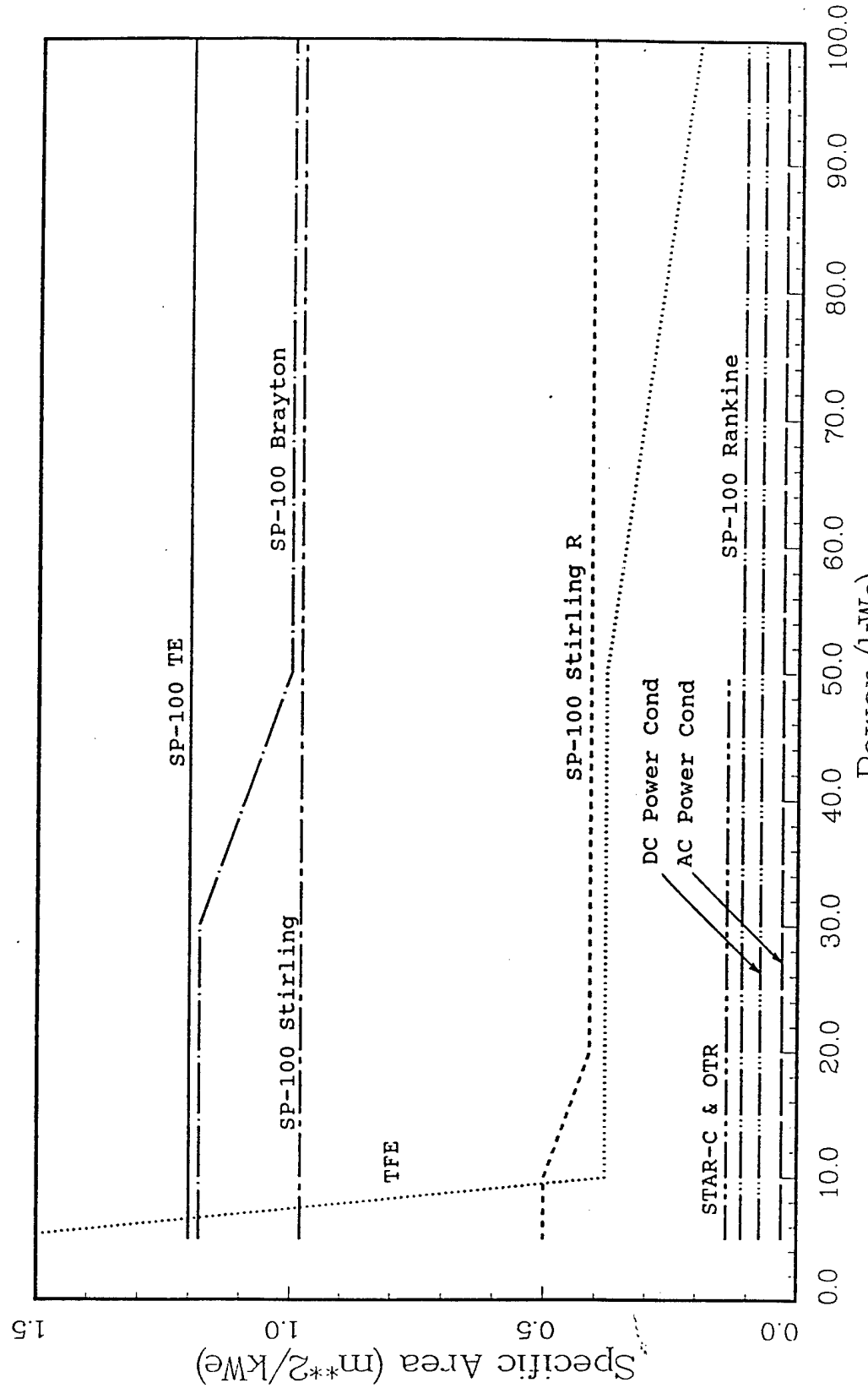

Figure 4.7: Specific Area Of Power System Radiators As A Function Of Power Level

5.0 Conclusions

Based on our mass and area estimates, which do not include the means to survive hostile threats, there is no compelling reason to choose one nuclear power system technology over another at power levels below 40 kW(e) until requirements become more firmly established. Differences in volume at launch and during operation may be more important than mass differences at the lower power levels. However, differences in power system masses become more significant as the required power increases further and further beyond the 40 to 60 kW(e) range. The near-term system that looks promising from the mass perspective at the higher power levels is the SP-100/Brayton system. In the far-term, substantial mass and area savings could be realized by going to a SP-100/Rankine power system.

Until requirements are more firmly defined, especially those dealing with survivability, and power systems are designed to meet these and many other specific satellite integration requirements, comparisons of power system concepts will remain mostly a matter of conjecture because many system attributes, including mass, may be altered dramatically by these requirements.

References

1. D. Boyle, "Space Nuclear Power for Military Applications," Presentation to Air Force Nuclear Mission Advisor Board, Air Force Weapons Laboratory, January 24, 1989.

2. Concept Definition Phase Of The STAR-C Thermionic Power System For The Boost Surveillance And Tracking System, GA Technologies Report GA-C18676, January 1987.

3. D. R. Gallup, The Scalability of OTR Space Nuclear Power Systems, Sandia National Laboratories Report SAND90-0163, March 1990.

4. TFE Verification Program Semiannual Report For The Period Ending April 30, 1989, GA Technologies Report GA-A19666, September 1989.

5. "SNAP/TFE Verification/'Topaz' Program Derivative Small Reactor Space Power Systems 10kWe/30kWe," Presentation to DOE/Air Force Small Reactor Committee, Space Power, Inc., October 21, 1987.

6. "Moderated In-Core Thermionic Space Reactors," Presentation to DOE/USAF Small Space Reactors Review Panel, GA Technologies, October 19, 1987.

7. SP-100 Project Integration Meeting (PIM), Viewgraph Presentation Volumes 1, 2, and 3, General Electric, July 19-21, 1988.

8. "AFWL Request For 10 kWe Point Design Flight Qualification Planning Information," Presentation to Air Force Space Technology Center, General Electric Astro Space, May 17, 1989.

9. Personal Communication, A. Marshall (Sandia National Laboratories) and B. McKissock (NASA Lewis Research Center), April 7, 1989.

10. See Pok Wong, William D. Jackson, William J. McKee, and E. J. Britt, "Low-voltage High Current Power Conditioning Module", AFWAL-TR-88-2019, Space Power Inc., June 1988.

11. A. Marshall, RSMASS: A Preliminary Reactor/Shield Mass Model For SDI Applications, Sandia National Laboratories Report SAND86-1020, August 1986.

12. A. Marshall, "Scaling Model For An Out-Of-Core Thermionic Power System," Sandia National Laboratories, Memo to L. Cropp, February 13, 1989.

13. A. Marshall, "Improvements To The STAR-C Model," Sandia National Laboratories, Memo to L. Cropp, February 24, 1989.

14. A. Marshall, "Further Improvements To STAR-C Shield Model," Sandia National Laboratories, Memo to L. Cropp, April 4, 1989.

15. A. Marshall, "Scaling Model For Liquid Metal Cooled Reactors (RSLM)," Sandia National Laboratories, Memo to L. Cropp, March 19, 1989.

16. A. Marshall, "Scaling Model For Thermionic Fuel Element Reactors (RSTFE)," Sandia National Laboratories, Memo to L. Cropp, April 11, 1989.

17. A. Pietsch and D. Brandes, "Advanced Solar Brayton Power Systems," Proceedings of the 24th Intersociety Energy Conversion Engineering Conference, pp 911-916, August 1989.

18. Personal Communication, L. Cropp (Sandia National Laboratories) and J. Dudenhoeffer (NASA Lewis Research Center), September 8, 1989.

19. E. Wahlquist, Letter to Col. C. Heimach (USAF Space Systems Division) re: Space Power System Masses, August 2, 1989.

20. Air Force Space Technology Center, Presentation to the Air Force Nuclear Mission Advisory Board, November 8, 1989.

21. Personal Communication, D. Gallup (Sandia National Laboratories) and W. Dawes (Sandia National Laboratories), November 10, 1989.

DISTRIBUTION

Note: DOE/OSTI, UC 700 59 copies.

Julio C. Acevedo
PSIO/NASA
Lewis Research Center
21000 Brookpark Rd.
Cleveland, OH 44135

Dr. C. A. Aeby
WL/NTC
Weapons Laboratory
Kirtland AFB, NM 87117

Lt. Col A. Alexander
AFSTC/SW
Kirtland AFB, NM 87117

Douglas Allen
W. J. Schafer Associates
1901 No. Ft. Myers Drive
Suite 800
Arlington, VA 22209

L. Amstutz
U.S. Army Belvoir RDE Ctr.
STRABE-FGE
Fort Belvoir, VA 22060-5606

Larry Atha
U.S. Army Strategic Defense Com.
106 Wynn Drive
Huntsville, AL 35807

Lt. Dale Atkinson
WL/NTCA
Weapons Laboratory
Kirtland AFB, NM 87117

General Electric
Attn: H. S. Bailey
6835 Via del Oro
San Jose, CA 95153

Rick R. Balthaser
RETD
U.S. Department of Energy
Albuquerque Operations Office
Albuquerque, NM 87115

C. Perry Bankston
California Institute of Technology
Jet Propulsion Laboratory
4800 Oak Grove Drive
MS 122-123
Pasadena, CA 91109

Major W. Barattino
WL/TAS
Kirtland Air Force Base
New Mexico 87117-6002

J. O. Barner
Battelle Pacific Northwest Laboratory
P. O. Box 999
Richland, WA 99352

D. Bartine
Oak Ridge National Laboratory
P. O. Box Y
Bldg 9201-3, MS-7
Oak Ridge, TN 37831

Ormon Bassett
W. J. Schafer Associates
1901 No. Ft. Myers Drive
Suite 800
Arlington, VA 22209

Ms. Kathleen Batke
NASA Lewis Research Center
Research/Technology Branch
21000 Brookpark Road
MS 3350
Cleveland, OH 44135

J. Beam
AFWRDC/POOS
Wright-Patterson Air Force Base
Ohio 45433

J. A. Belisle
Manager, Energy Programs
Grumman Aerospace Corp.
MS B20-05
Bethpage, NY 11714

C. Bell
Los Alamos National Laboratory
P.O. Box 1663
MS-F611
Los Alamos, NM 87545

RP/Gary Bennett
NASA Headquarters
600 Independence Ave.
Washington, DC 20546

David Bents
NASA Lewis Research Center
21000 Brookpark Road
MS 301-5, Rm. 101
Cleveland, OH 44135

J. A. Bernard
Massachusetts Institute of Technology
1328 Albany Street
Cambridge, MA 02139

Dave Berwald
Grumman Aerospace Corporation
MS B20-05
Bethpage, NY 11714

F. Best
Assistant Professor
Texas A&M University
Nuclear Engineering Dept.
College Station, TX 77843-3133

Mark Bezik
NASA Lewis Research Center
MS 3160
21000 Brookpark Rd.
Cleveland, OH 44135

Samit K. Bhattacharyya
Argonne National Laboratory
9700 So. Cass Avenue
Bldg. 207
Argonne, IL 60439-4841

H. S. Bloomfield
Program Manager
NASA Lewis Research Center
MS 301-5, Rm. 103
21000 Brookpark Road
Cleveland, OH 44135

Ron Boatwright MS-L-8030
Attn: Document Control
Martin Marietta Space Systems
P O Box 179
Denver, CO 80201

Richard J. Bohl
Los Alamos National Laboratory
MS K560
P. O. Box 1663
Los Alamos, NM 87545

James Bolander
NASA Lewis Research Center
21000 Brookpark Road
Cleveland, OH 44135

William Borger
AFWRDC/POOA
Aeronautical Laboratory
Wright Patterson AFB
Ohio 45433

S. Borowski
NASA Lewis Research Center
MS: 501-6
21000 Brookpark Road
Cleveland, OH 44135

D. Bouska
U.S. Army Strategic Defense Command
106 Wynn Drive
Huntsville, AL 35807

T. Bowden
Brookhaven National Laboratory
P. O. Box 155
Upton, NY 11973

Robert Boyle
Garrett Fluid Systems Co.
P. O. Box 5217
Phoenix, AZ 85010-5217

Mr. Dick Bradshaw
CSSD-H-SAV
US Army Strategic Defense Command
106 Wynn Drive
P. O. Box 1500
Huntsville, AL 35807-3801

Jerry Bueck
W. J. Schafer Associates
2000 Randolph Road, SE
Suite 205
Albuquerque, NM 87106

Wade Carroll
U.S. Department of Energy
NE 52
Germantown Building
Washington, DC 20545

R. D. Casagrande
General Electric
Astro Systems
P. O. Box 8555
Philadelphia, PA

L. Caveny
SDIO/IST
Washington, DC 20301-7100

B. Chadsey
SAIC
1710 Goodridge Drive
McLean, VA 22101

T. S. Chan
General Electric
Astro Systems/SCO
P. O. Box 8555
35T15, Bldg. 20
Philadelphia, PA 19101

John W. H. Chi
Westinghouse Electric Corp.
Advanced Energy Systems
P.O. Box 158
Madison, PA 15663

W. Chiu
General Electric
Space Systems Division
Valley Forge Space Center
P. O. Box 8555
Rm. 35T20, Bldg. 20
Philadelphia, PA 19101

Paul Chivington
TRW, Inc.
Suite 200
2340 Alamo, Se
Albuquerque, NM 87106

Lynn Cleland
Lawrence Livermore National Laboratory
P.O. Box 808
MS L-144
Livermore, CA 94550

Robert Cooper
MS MS-241
Aerospace Corporation
P. O. Box 92957
Los Angeles, CA 90009-2957

E. P. Coomes
Battelle Pacific Northwest Laboratory
P. O. Box 999
Richland, WA 99352

Carl Cox
Westinghouse Hanford
MS C-27
P.O. Box 1970
Richland, WA 99352

Cecil Crews
MS M5-614
Aerospace Corporation
P. O. Box 92957
Los Angeles, CA 90009-2957

J. Crissey
W. J. Schafer Associates
1901 No. Ft. Myers Drive
Suite 800
Arlington, VA 22209

R. Dahlberg
General Atomics
P. O. Box 85608
San Diego, CA 92138

Dr. Gracie E. Davis
RAEE
HQ Defense Nuclear Agency
6801 Telegraph Road
Alexandria, VA 22213

R. Dewitt
Naval Surface Weapons Ctr.
Code F-12
Dahlgren, VA 22448-5000

N. Diaz
INSPI
202 NSC
University of Florida
Gainesville, FL 32611

P. J. Dirkmaat
U.S. Department of Energy/Idaho
785 DOE Place
Idaho Falls, ID 83402

M. P. Dougherty
Martin Marietta Corporation
Astronautics Group
Space Systems
P.O. Box 179
Denver, CO 80201

Rudy Duscha
NASA Lewis Research Center
PSIO
21000 Brookpark Rd.
Cleveland, OH 44135

Mr. Richard Dudney
CSSD-H-YA
US Army Strategic Defense Command
106 Wynn Drive
P. O. Box 1500
Huntsville, AL 35807-3801

D. S. Dutt
Manager, Fuel Design
Westinghouse Hanford
Engineering Development Lab.
P. O. Box 1970
Richland, WA 99352

G. Edlin
U.S. Army Strategic Defense Cm.
106 Wynn Drive
Huntsville, AL 35807

M. El-Genk
University of New Mexico
Chemical and Engineering Department
Albuquerque, NM 87131

Jeffrey George
MS 501-6
NASA Lewis Research Center
21000 Brookpark Road
Cleveland, OH 44135

Dr. David M. Ericson, Jr.
ERCE
7301-A Indian School Rd., NE
Albuquerque, NM 87110

D. Escher
TRW
One Space Park
Redondo Beach, CA 90278

J. Farber
Defense Nuclear Agency
RAEV
6801 Telegraph Road
Alexandria, VA 22310-3398

G. Farbman
Westinghouse
Advanced Energy Systems Division
P. O. Box 158
Madison, PA 15663

M. Firmin
Aerospace Corporation
P.O. Box 9113
Albuquerque, NM 87119

T. Fitzgerald
TRW
One Space Park
Redondo Beach, CA 90278

Terry Flannagan
JAYCOR
11011 Torreyana Road
P.O. Box 85154
San Diego, CA 92138-9259

Dr. Dennis Flood
NASA Lewis Research Center
Mail Stop: 302-1
2100 Brookpark Road
Cleveland, Ohio 44135

J. Foster
Defense Nuclear Agency
RAEV
6801 Telegraph Road
Alexandria, VA 22310-3398

E. P. Framan
California Inst. of Technology
Jet Propulsion Lab.
4800 Oak Grove Drive
MS 301-285
Pasadena, CA 91109

Dr. Mike Frankel
SPAS
HQ Defense Nuclear Agency
6801 Telegraph Road
Alexandria, VA 22213

Robert Franklin
U.S. Army Strategic Defense Cm.
106 Wynn Drive
Huntsville, AL 35807

Bob Gardner
Mission Research Corporation
1720 Randolph Road, SE
Albuquerque, NM 87106-4245

Dr. James Gee
MS M7-633
Aerospace Corporation
P. O. Box 92957
Los Angeles, CA 90009-2957

Jeffrey George
MS: 501-6
NASA Lewis Research Center
21000 Brookpark Rd.
Cleveland, OH 44135

R. Giellis
Martin Marietta Corp.
P. O. Box 179
MS 0484
Denver, CO 80201

Bruce Glasgow
R1/1070
TRW-ATD
One Space Park
Redondo Beach, CA 90278

Capt. J. Gray
WL/NTCA
Weapons Laboratory
Kirtland AFB, NM 87117

R. Gray
RADC/OCTP
Griffis Air Force Base
New York 13441

R. Gripshoven
Naval Surface Weapons Center
F12
Dahlgren, VA 22448-5000

R. L. Hammel
Product Line Manager
Spacecraft Engineering Division
TRW
One Space Park
Bldg. R-4/2190
Redondo Beach, CA 90278

R. Hammond
SDIO/DE
Washington, DC 20301-7100

W. R. Hardie
Deputy Group Leader
Los Alamos National Laboratory
MS F611
P. O. Box 1663
Los Alamos, NM 87545

Neal Harold
AFWAL/POOC-1
Wright-Patterson AFB
Ohio 45433-6563

Mr. Charlie D. Harper
CSSD-H-YA
US Army Strategic Defense Command
106 Wynn Drive
P. O. Box 1500
Hunstville, AL 35807-3801

Dr. M. Harrison
WL/NTCA
Weapons Laboratory
Kirtland AFB, NM 87117

S. Harrison
Office of Science & Technology
Executive Office of the President
Mailing Room 5013
New Executive Office Bldg.
Washington, DC 20506

J. K. Hartman
U. S. Department of Energy
San Francisco Operations Office
1333 Broadway Avenue
Oakland, CA 94612

L. Hatch
Rasor Associates
253 Humboldt Ct.
Sunnyvale, CA 94089

Col. C. Heimach
U. S. Air Force
SD/XR
P.O. Box 92960 WPC
Los Angeles AFB
CA 90009-2960

I. Helms
U. S. Department of Energy
NE-54
Washington, DC 20545

Mr. R. Herndon
AFSTC/SWL
Kirtland AFB, NM 87117

Lt. Col. C. Hill
SDIO/INK
Pentagon, Rm 1E178
Washington, DC 20301-7100

J. Hipp
S-Cubed
2501 Yale Blvd., SE
Suite 300
Albuquerque, NM 87106

E. E. Hoffman
U. S. Department of Energy
Oak Ridge Operations Office
P. O. Box E
Oak Ridge, TN 37830

H. W. Hoffman
Oak Ridge Nat'l Lab.
P.O. Box X
Oak Ridge, TN 37831

K. W. Hoffman
Air Force Foreign
Technology Division
TDTQ
Wright-Patterson AFB
Ohio 45433

R. L. Holton
U.S. Department of Energy
ALO/ETD
P.O. Box 5400
Albuquerque, NM 87115

J. L. Hooper
U. S. Department of Energy
Chicago Operations Office
9800 So. Cass Avenue
Argonne, IL 60439

CNSE/Capt. Howard
Space Systems Division
P. O. Box 92960
Worldway Postal Center
Los Angeles, CA 90009-2960

A. Huber
Air Force Space Technology Center
XLP
Kirtland Air Force Base
New Mexico 87117-6008

Dr. T. Hyder
Auburn University
202 Sanform Hall
Auburn, AL 36849-3501

D. E. Jackson
BDM Corporation
1801 Randolph Rd., SE
MS BV-24
Albuquerque, NM 87106

Jerry Jaggers
Attn: Document Control
for Bldg. 593
Lockheed Missiles and
Space Co. Inc.
P O Box 3504
Sunnyvale, CA 94088

Frank Jankowski
WL/TAPN
Kirtland AFB, NM 87117

Marshall Jew (MS: A02-105)
Grumman Aerospace Corporation
CDC (Ms: A04-35)
Bethpage, NY 11714

B. M. Johnson
Batelle Pacific Northwest Lab.
P.O. Box 999
Richland, WA 99352

R. Johnson
Rocket Dyne
HB-13
6633 Canoga Ave.
Canoga Park, CA 91303

A. Juhasz
NASA Lewis Research Center
MS 301-5, Rm. 101
21000 Brookpark Road
Cleveland, OH 44135

Col. John A. Justice
WL/NTN
Weapons Laboratory
Kirtland AFB, NM 87117

Ehsan Kahn
BDM Corp.
7915 Jones Branch Dr.
MS West Brach 5B37
McLean, VA 22102-3396

Robert Karcher, MS EA-22
Rockwell Int'l Space Transportation
Systems Division
12214 Lakewood Blvd.
Downey, CA 90241

W. Y. Kato
Deputy Chairman
Brookhaven National Laboratory
P. O. Box 155
Upton, NY 11973

D. Kelleher
Technical Director
Advanced Technology Division
AFWRDC/AW
Kirtland Air Force Base
New Mexico 87117

Peter Kemmey
DARPA
1400 Wilson Blvd.
Arlington, VA 22209

Lt. E. B. Kennel
AFWRDC/POOS
Bldg. 450
Wright Patterson AFB
Ohio 45433

K. Kennerud
Boeing Company
Boeing Aerospace System
P.O. Box 3707
Seattle, WA 98124

O. F. Kimball
Oak Ridge Nat'l Lab.
P.O. Box 2009
Bldg. 4508, MS 080
Oak Ridge, TN 37831-6080

F. King
U. S. Army Defense Command
106 Wynn Drive
Huntsville, AL 35807

W. L. Kirk
Los Alamos National Laboratory
P. O. Box 1663
Los Alamos, NM 87545

A. Klein
Oregon State University
Dept. of Nuclear Engineering
Corvallis, Oregon 97331

J. Krupa
U. S. Department of Energy
SAN-ACR Division
1333 Broadway
Oakland, CA 94612

K. D. Kuczen
Argonne National Laboratory
97000 So. Cass Avenue
Argonne, IL 60439

Gerald Kulcinski
University of Wisconsin
Fusion Technology Institute
1500 Johnson Drive
Madison, WI 53706-1687

A. S. Kumar
University of Missouri-Rolla
Department of Nuclear Energy
220 Engineering Research Lab.
Rolla, MO 65401-0249

W. Lambert
U. S. Department of Energy
SAN-ACR Division
1333 Broadway
Oakland, CA 94612

Dick Lancashire
PSIO/NASA
Lewis Research Center
21000 Brookpark Rd.
Cleveland, OH 44135

Lt. Col. F. Lawrence
HQ ASFPACECOM/XPXIS
Peterson Air Force Base
Colorado 80914-5001

R. J. LeClaire
Los Alamos National Laboratory
P. O. Box 1663
MS F611
Los Alamos, NM 87545

CNIS/Lt. Col. J. Ledbetter
Space Systems Division
P. O. Box 92960
Worldway Postal Center
Los Angeles, CA 90009-2960

J. P. Lee
U. S. Department of Energy
MS MA-206
Washington, DC 20545

Dr. James H. Lee, Jr.
SDIO/TNK
The Pentagon
Washington, DC 20301-7100

Lt. Col. R. X. Lenard
SDIO/KE
The Pentagon
Washington, DC 20301-7100

S. Levy
U. S. Army ARDC
Building 329
Picatinny Arsenal
New Jersey 87806-5000

R. A. Lewis
Argonne Nat'l Lab.
9700 So. Cass Avenue
Argonne, IL 60439

Larry Long
Westinghouse R&D
1310 Beulah Road
Bldg. 501-3Y56
Pittsburgh, PA 15235

L. H. Luessen
Naval Surface Weapons Center
Code F12
Dahlgren, VA 22448-5000

Bruce MacCabee
R/42
Naval Surface Weapons Laboratory
White Oaks
Silver Springs, MD 20910

Phil Mace
W. J. Schafer Associates
1901 North Ft. Myers Drive
Suite 800
Arlington, VA 22209

P. Mahadevan
MS M7-597
Aerospace Corporation
PO Box 92957
Los Angeles, CA 90009-2957

T. Mahefky
Group Leader, Thermal Systems
AFWRDC
Aeronautical Laboratory
Wright Patterson Air Force Base
Ohio 45433

B. J. Makenas
Westinghouse Hanford Company
P. O. Box 1970
Richland, WA 99352

P. Margolis
Aerospace Corporation
P. O. Box 92957
El Segundo, CA 90009

Lee Mason
NASA Lewis Research Center
MS: 501-6
21000 Brookpark Road
Cleveland, OH 44135

L. D. Massie
AFWRDC/POOC-1
Aeronautical Laboratory
Bldg. 450
Wright-Patterson AFB
Ohio 45433

Bill Matoush
AFSPACESOM/XPXY
Peterson AFB
Colorado Springs, CO 80915-5001

Maj. Tom McDowell
SDIO/INK
Pentagon, Rm 1E178
Washington, DC 20301-7100

Glen McDuff
Texas Tech. University
Dept. of Electrical Engr.
Lubbock, TX 79409

Barbara McKissock
NASA Lewis Research Center
MS 301-5
21000 Brookpark Road
Cleveland, OH 44135

D. McVay
United Technologies
International Fuel Cells
195 Governor's Highway
So. Windsor, CT 06074

M. A. Merrigan
Los Alamos National Laboratory
P. O. Box 1663
Los Alamos, NM 87545

Ira Merritt
CSSD-H-LS
US Army Strategic Defense Command
106 Wynn Drive
P. O. Box 1500
Huntsville, AL 35807-3801

B. Meyers
Naval Space Command
Dahlgren, VA 22448

J. Metzger
Los Alamos National Laboratory
P. O. Box 1663
Los Alamos, NM 87545

Tom Miller
ASAO/NASA
Lewis Research Center
21000 Brookpark Rd.
Cleveland, OH 44135

J. Mims
S-Cubed
2501 Yale Blvd., SE
Suite 300
Albuquerque, NM 87106

J. F. Mondt
Deputy Project Manager
California Institute of Technology
Jet Propulsion Laboratory
4800 Oak Grove Drive
Pasadena, CA 91109

Capt. J. Moody
AFSTC/SWW
Kirtland AFB, NM 87117

J. C. Moyers
Oak Ridge National Laboratory
P. O. Box Y
Bldg. 9201-3, MS-7
Oak Ridge, TN 37831

D. M. Mulder
AFWL/TAPN
Kirtland Air Force Base
New Mexico 87117-6008

Mr. J. Mullis
WL/NTCA
Weapons Laboratory
Kirtland AFB, NM 87117

I. T. Myers
NASA Lewis Research Center
MS 301-2, Rm. 116
21000 Brookpark Road
Cleveland, OH 44135

Joseph Nainiger
MS 501-6
NASA Lewis Research Center
21000 Brookpark Road
Cleveland, OH 44135

D. F. Nichols
AFWL/TAPN
Kirtland AFB
NM 87117-6008

J. P. Nichols
Oak Ridge National Laboratory
Bldg. K-1030, Room 110
P. O. Box 2003
Oak Ridge, TN 37831-7312

M. Nikolich
W. J. Schafer Associates
1901 No. Ft. Myers Drive
Suite 800
Arlington, VA 22209

Commander R. Nosco
Naval Space Command
Dahlgren, VA 22448

George Novak
Cost Analysis Org.
NASA/Lewis Research Center
21000 Brookpark Rd.
Cleveland, OH 44135

Capt. P. D. Nutz
USAF-SD/CNSD
P.O. Box 92960
LA-AFS
Los Angeles, CA 90009-2960

Tuong Nguyen
MS FB25
Rocketdyne
6633 Canoga Ave.
Canoga Park, CA 91303

C. Oberly
AFWRDC/POOC-1
Wright-Patterson AFB
Ohio 45433

M. Olszewski
Oak Ridge National Laboratory
P. O. Box Y
Oak Ridge, TN 37831

D. Palac
NASA Lewis Research Center
MS: 501-6
21000 Brookpark Road
Cleveland, OH 44135

Dr. D. Payton
EOS Technologies Inc.
200 Lomas NW, Suite 1121
Albuquerque, NM 87102

Capt. G. Peredo
U. S. Air Force
SD/XR
P.O. Box 92960 WPC
Los Angeles AFB
CA 90009-2960

Ed Peterson
Code 4611
Naval Research Laboratory
4555 Overlook Drive
Washington, DC 20375-5000

W. Portnoy
Texas Tech University
Dept of Electrical Engineering
Lubbock, TX 79409

J. Powell
Office of Reactor Systems
Brookhaven National Laboratory
MS 820M, Bldg. 701, Level 143
P. O. Box 155
Upton, NY 11973

J. L. Preston, Jr.
United Technologies
International Fuel Cells
195 Governor's Highway
South Windsor, CT 06074

Eric Proust
Commissariat A L'Energie Atomique
Dept. des Etudes Mechaniques
et Thermiques
33 Rue de La Federation
75015 Paris
FRANCE

Lt. Col. H. Pugh
AFSTC/SWL
Kirtland AFB, NM 87117

C. Purvis
NASA Lewis Research Center
MS 302-1, Rm. 101
21000 Brookpark Road
Cleveland, OH 44135

C. Quinn
U. S. Department of Energy
ALO/ETD
P. O. Box 5400
Albuquerque, NM 87115

William A. Ranken
Los Alamos National Laboratory
Mail Stop: E552
P. O. Box 1663
Los Alamos, NM 87545

N. Rasor
Rasor Associates
253 Humboldt Ct.
Sunnyvale, CA 94089

D. Reid
Los Alamos National Laboratory
MS H811
P. O. Box 1663
Los Alamos, NM 87545

CNBSS/Maj. L. Rensing
Space Systems Division
P. O. Box 92960
Worldway Postal Center
Los Angeles, CA 90009-2960

Dick Renski
AFWRDC/AA
Wright-Patterson AFB
Ohio 45433

J. R. Repp
Westinghouse R&D
1310 Beulah Road
Bldg. 501-3Y56
Pittsburgh, PA 15235

W. H. Roach
S-Cubed
2501 Yale Blvd., SE
Suite 300
Albuquerque, NM 87106

Carlos D. Rodriquez
ASAO/NASA
Lewis Research Center
21000 Brookpark Rd.
Cleveland, OH 44135

Frank Rose
Auburn University
Space Power Institute
231 Leach Center
Auburn, AL 36849-3501

J. H. Saloio
ERCE
7301-A Indian School Road, NE
Albuquerque, NM 87110

S. L. Samuelson
U. S. Department of Energy
San Francisco Operations Office
1333 Broadway Avenue
Oakland, CA 94612

R. T. Santoro
Oak Ridge National Laboratory
P. O. Box 22008
Oak Ridge, TN 37831-6363

Mike Saunders
Booz-Allen and Hamilton Inc.
4330 East-West Highway
Bethesda, MD 20814

L. Schmid
Assistant Project Manager
Battelle Pacific Northwest Lab.
P. O. Box 999
Richland, WA 99352

Paul Schmitz
MS: 301-5
NASA Lewis Research Center
21000 Brookpark Road
Cleveland, OH 44135

Lt. Col. Schneider
WL/NTC
Weapons Laboratory
Kirtland AFB, NM 87117

Col. Garry Schnelzer
SDIO/SATKA
Washington, DC 20301-7100

A. D. Schnyer
NASA Headquarters
Room 600, Code: RP
600 Independence Ave., SW
Washington, DC 20546

Col. J. Schofield
SDIO/SY
Washington, DC 20301-7100

J. Scholtis
Directorate of Nuclear Safety
AFISC/SN
DET 1, AFISC/SNRA
Kirtland AFB
New Mexico 87117-5000

M. J. Schuller
WL/TAPN
Kirtland Air Force Base
New Mexico 87117-6008

G. Schwarze
NASA Lewis Research Center
MS 301-2, Rm. 117
21000 Brookpark Road
Cleveland, OH 44135

Jim Scott
Los Alamos National Laboratory
Mail Stop: E552
P. O. Box 1663
Los Alamos, NM 87545

Clarence Severt
AFWRDC/POOC-1
Wright-Patterson AFB
Ohio 45433-6563

Lt. Col. John Seward
WRDC/AAW
Wright Patterson Air Force Base
Ohio 45433

D. C. Sewell
DCSCON Consulting
4265 Drake Court
Livermore, CA 94550

C. Sharn
SDIO/SY
Washington, DC 20301-7100

B. J. Short
Babcock & Wilcox
Nuclear Power Division
3315 Old Forest Road
P.O. Box 10935
Lynchburg, VA 24506-0935

M. Simon-Tov
Oak Ridge Nat'l Lab.
Bldg. 9201-3, MS-7
Oak Ridge, TN 37831

CNIWT/Capt. Simpson
Space Systems Division
P. O. Box 92960
Worldway Postal Center
Los Angeles, CA 90009-2960

Dr. B. K. Singaraju
WL/NTCA
Weapons Laboratory
Kirtland AFB, NM 87117

Henry Smith
Nichols Research Corp.
4040 So. Memorial Pkwy
Huntsville, AL 35802

John Smith
NASA Lewis Research Center
MS 301-5
21000 Brookpark Road
Cleveland, OH 44135

S. Solomon
Aerospace Corp.
P. O. Box 92957, MS: M1-131
Los Angeles, CA 90009-2957

R. J. Sovie
NASA Lewis Research Center
MS 301-5, Rm. 105
21000 Brookpark Road
Cleveland, OH 44135

O. Spurlock
NASA Lewis Research Center
MS 501-6
21000 Brookpark Road
Cleveland, OH 44135

G. Staats
U. S. Department of Energy
Pittsburgh Energy Tech. Center
PM-20
P. O. Box 18288
Pittsburgh, PA 15236

M. L. Stanley
EG&G Idaho, Inc./INEL
P. O. Box 1625
Idaho Falls, ID 83415

Steve Stevenson
NASA Lewis Research Center
ASAO
21000 Brookpark Rd.
Cleveland, OH 44135

D. C. Straw
W. J. Schafer Associates
2000 Randolph Road, SE
Suite 205
Albuquerque, NM 87106

O. Spurlock
NASA Lewis Research Center
MS: 501-6
21000 Brookpark Road
Cleveland, OH 44135

T. P. Suchocki
Los Alamos National Laboratory
P. O. Box 1663
Los Alamos, NM 87545

L. H. Sullivan
Los Alamos National Laboratory
P. O. Box 1663
Los Alamos, NM 87545

A. Sutey
Spacecraft Subsystems
Boeing Company
P. O. Box 999
MS 8K-30
Seattle, WA 98124-2499

D. W. Swallom
AVCO Research Laboratory
2385 Revere Beach Parkway
Everett, MA 02149

Major P. Talty
HQ USAF/RD-D
Washington, DC 20330-5042

Owen Taylor
Westinghouse R&D
1310 Beulah Road
Bldg. 501-3Y56
Pittsburgh, PA 15235

Charles Terrell
WL/TA
Kirtland AFB,
NM 87117-6008

R. Thibodeau
AFWRDC/POOC-1
Bldg. 450
Wright Patterson Air Force Base
Ohio 45433

J. C. Trocciola
United Technologies
International Fuel Cells
195 Governor's Highway
South Windsor, CT 06074

V. C. Truscello
California Institute of Technology
Jet Propulsion Laboratory
4800 Oak Grove Drive
Bldg. 264-770
Pasadena, CA 91109

John Uecke
S-Cubed
Suite 300
2501 Yale Blvd., SE
Albuquerque, NM 87106

T. H. Van Hagan
General Atomics
10955 John Jay Hopkins Dr.
P. O. Box 85608
San Diego, CA 92121-1194

G. B. Varnado
Int'l Energy Associates Ltd.
1717 Louisiana NE
Suite 202
Albuquerque, NM 87110

R. Verga
SDI Organization
The Pentagon
Washington, DC 20301-7100

D. C. Wade
Applied Physics Division
Argonne National Laboratory
9700 So. Cass Avenue
Argonne, IL 60439

John Wagner
SAIC
2109 Air Park Road, SE
Albuquerque, NM 87106

E. J. Wahlquist
U. S. Department of Energy
NE-54
F415/GTN
Germantown, MD 20545

C. E. Walter, P.E.
Lawrence Livermore National Lab.
P. O. Box 808
MS L-144
Livermore, CA 94550

J. Warren
U. S. Department of Energy
NE-52
GTN
Germantown, MD 20545

C. W. Watson
Los Alamos National Laboratory
MS F607
P. O. Box 1663
Los Alamos, NM 87545

Robert C. Webb
RAEE
HQ Defense Nuclear Agency
6801 Telegraph Road
Alexandria, VA 22213

R. Weed
Nichols Research Corporation
2340 Alamo SE
Suite 105
Albuquerque, NM 87106

Eric Wennas
JAYCOR
11011 Torreyana Road
P. O. Box 85154
San Diego, CA 92138-9259

J. R. Wetch
President
Space Power, Inc.
621 Riverside Pkwy.
San Jose, CA 95134

J. F. Wett
Space & Defense Program
Westinghouse
Advanced Energy Systems Div.
Route 70, Madison Exit
Madison, PA 15663

Dan Whittener
U.S. Army Strategic Defense Cm.
106 Wynn Drive
Huntsville, AL 35807

R. D. Widrig
Human Factors Projects
Battelle Pacific Northwest Laboratory
P. O. Box 999
Richland, WA 99352

F. W. Wiffen
Oak Ridge National Laboratory
P. O. Box Y
Bldg. 9201-3, MS-7
Oak Ridge, TN 37831

Major J. Wiley
Naval Space Command
N5
Dahlgren, VA 22448

Robert Wiley
5998 Camelback Lane
Columbia, MD 21045

E. L. Wilkinson
U. S. Army Strategic Defense Command
106 Wynn Drive
Huntsville, AL 35807

Dr. Ken Williams
SAIC
2109 Air Park Road, SE
Albuquerque, NM 87106

N. Wilson
U. S. Army Lab. Com.
SLKET/ML
Pulse Power Technology Branch
Ft. Monmouth, NJ 07703-5000

Jerry Winter
NASA Lewis Research Center
21000 Brookpark Road
Cleveland, OH 44135

William Wright
Ballena Systems Corporation
1150 Ballena Blvd., Suite 210
Alameda, CA 94501

T. S. Wuchte
AFWL/TAPN
Kirtland AFB
NM 87117-6008

E. R. Zercher
Martin Marietta Corporation
MS L8060
P. O. Box 179
Denver, CO 80201

J. Zielinski
U. S. Department of Energy
SAN-ACR Division
13333 Broadway
Oakland, CA 94612

G. L. Zigler
Science & Engineering Associates
6301 Indian School NE
Albuquerque, NM 87110

Internal Distribution

P. Jalichandra
Loral Electro-Optical Systems
Lasers & Light Sources Dept.
300 N. Halstead St.
Pasadena, CA 91109

1200 J. P. Van Devender
1230 J. Powell
1233-1 A. Sharpe
1236 J. Zawadkas
1240 K. Prestwich
1248 M. Buttram
1270 R. Miller
1271 M. Clauser
1512 D. Rader
1810 G. Kepler
1830 M. Davis
1832 W. Jones
1840 R. Eagan
2110 R. Bair
2150 E. Graham, Jr.
2560 J. Cutchen
2175 J. Meyer
2330 J. Stichman
2336 E. Nava
2346 B. O'Nan
3141 S. A. Landenberger (5)
3151 W. L. Klein (3)
3141-1 C. L. Ward for DOE/OSTI (8)
6201 M. Edenburn
6400 D. J. McCloskey
6410 D. Dahlgren
6420 W. Gauster
6421 P. Pickard
6422 J. Brockmann
6450 T. Schmidt
6453 J. Philbin
6460 J. Walker
6461 G. Allen
6461 W. McCulloch
6461 P. McDaniel
6461 F. Wyant
6461 L. Sanchez
6461 D. Dobranich
6461 V. Dandini
6472 D. McCloskey, Actg.
6465 W. Champion
6465 D. Gallup (20)
6465 D. Monroe
6465 R. Pepping
6465 R. Peters
6474 W. Wheelis
6690 D. Berry
6900 A. W. Snyder
8400 R. Wayne
8442 M. Stoddard
8524 J. A. Wackerly
9000 R. Hagengruber
9010 W. Hines
9014 J. Keizur
9014 R. Zazworsky
9015 R. Preston
9100 R. Clem
9110 P. Stokes
9140 D. Rigali
9320 M. Navatril
9321 B. Boyer
9340 W. Beezhold
9342 L. Choate
9350 J. Renken
9351 F. Hartman

Org.	Bldg.	Name	Rec'd by	Org.	Bldg.	Name	Rec'd by